UNIVERSITY OF CALIFORNIA,
IRVINE

Mathematical and Computational Models of Virus Dynamics

DISSERTATION

submitted in partial satisfaction of the requirements
for the degree of

DOCTOR OF PHILOSOPHY

in Ecology and Evolutionary Biology

by

Dustin Phan

Dissertation Committee:
Professor Dominik Wodarz, Chair
Professor Laurence Mueller
Associate Professor Jose Ranz

2015

TABLE OF CONTENTS

Page

LIST OF FIGURES iii

LIST OF TABLES v

ACKNOWLEDGMENTS vi

CURRICULUM VITAE vii

ABSTRACT OF THE DISSERTATION viii

CHAPTER 1: Introduction
- 1.1 The multiple infection of cells by viruses 2
- 1.2 Oncolytic viruses for the eradication of drug resistant cancer cells 6

CHAPTER 2: Modeling multiple infection of cells by virus
- 2.1 Introduction 11
- 2.2 Basic ODE models of multiple infection 13
- 2.3 Virus parameters are independent of infection multiplicity 16
- 2.4 Virus parameters depend on infection multiplicity 17
- 2.5 Discussion and Conclusion 20

CHAPTER 3: The role of multiple infection on competition dynamics
- 3.1 Introduction 22
- 3.2 ODE model of competition dynamics in the context of multiple infection 24
- 3.3 Virus parameters are independent of infection multiplicity 28
- 3.4 Virus parameters depend on infection multiplicity 32
- 3.5 Effect of the infection cascade length 32
- 3.6 Effect of space 34
- 3.7 Discussion and Conclusion 38

CHAPTER 4: A computational model of oncolytic viruses for the eradication of drug resistant cancer cells
- 4.1 Introduction 42
- 4.2 Agent-based model of oncolytic virus infection 45
- 4.3 Dynamics of drug resistant versus drug sensitive cancer cells with treatment 47
- 4.4 Combination therapy during early growth phase 52
- 4.5 Discussion and Conclusion 57

CHAPTER 5: Summary and Conclusions 61

REFERENCES 64

LIST OF FIGURES

		Page
Figure 1.1	Schematic diagram illustrating the basic principles of models of multiple infection of cells by viruses.	5
Figure 1.2	Schematic demonstrating the preferential replication and killing of oncolytic viruses in (a) cancer and (b) normal cells.	9
Figure 2.1	Distribution of the number of cells infected with *I* viruses, according to model (1) where the rate of virus production does not depend on infection multiplicity.	17
Figure 2.2	Equilibrium number of cells as a function of the infection multiplicity, according to model (1).	18
Figure 3.1	Outcomes of the competition model (2). (a) Competitive exclusion. (b) Coexistence.	30
Figure 3.2	Outcome of competition in model (2), depending on parameters that determine the rate of virus spread, and the parameter *c*, which describes the relative strength of intracellular competition among the two virus strains.	31
Figure 3.3	Dependence of the competition outcome in model (2) on the length of the infection cascade, *n*.	33
Figure 3.4	(a) Competition in spatial (nearest neighbor) versus non-spatial (mass-action) settings, using the agent-based model described in the text. (b) Reason for the larger extinction region in the spatial simulation.	37
Figure 4.1	The growth of drug sensitive and drug resistant mutants in the (a) absence and (b, c) presence of an oncolytic virus.	49
Figure 4.2	Simulation demonstrating the effect of stochasticity on the success of drug therapy.	50

Figure 4.3 The effect of oncolytic virus infection rate on (a) the average fraction of time that the mutant is extinct and (b) the success of drug therapy. 52

Figure 4.4 Simulation demonstrating the effect of stochasticity on the success of the sequential combination of oncolytic virus therapy and drug treatment during the quadratic growth phase. 53

Figure 4.5 The effect of oncolytic virus infection rate on (a) the average fraction of time that the mutant is extinct and (b) the success of drug therapy during the quadratic growth phase. 56

LIST OF TABLES

		Page
Table 2.1	Parameters for basic ODE model of multiple infection.	15
Table 3.1	Parameters for ODE model of multiple infection with competition dynamics.	25
Table 3.2	Parameters for agent based model of multiple infection with spatial dynamics.	35
Table 4.1	Parameters for spatial agent based model of oncolytic virus therapy.	47

ACKNOWLEDGMENTS

First and foremost, I would like to thank my committee chair and advisor Professor Dominik Wodarz. Without his immense patience and guidance over the preceding years, this dissertation would not have been possible. His wealth of knowledge and experience has provided the foundation for this interdisciplinary work.

I would also like to thank my committee members Professors Laurence Mueller and Jose Ranz, who ensured I understood the biological contexts of all my projects. They have always provided constructive suggestions, valuable discussions, and unique insights. I thank them for their service on my committee.

I also express my gratitude to Professor John Lowengrub of the Department of Mathematics for introducing me to the field computational biology.

Finally, I would like to thank the Department of Ecology and Evolutionary Biology, the Mathematical, Computational, and Systems Biology Program, and the Center for Complex Biological Systems for their support.

CURRICULUM VITAE

Dustin Phan

2009	B.S. in Applied and Computational Mathematics. University of California, Irvine
2009-2010	Mathematical, Computational, and Systems Biology Gateway Program University of California, Irvine
2010-2015	Graduate Student Researcher, Ecology and Evolutionary Biology University of California, Irvine
2010-2015	Teaching Assistant, Department of Ecology and Evolutionary Biology University of California, Irvine
2015	Ph.D. in Ecology and Evolutionary Biology University of California, Irvine

FIELD OF STUDY

Computational Biology, Population Dynamics

PUBLICATIONS

D. Phan and D. Wodarz, Modeling multiple infection of cells by viruses: challenges and insights. Mathematical Biosciences **264** (2015) 21-28.

UNDERGRADUATE THESIS

D. Phan, A discrete cellular automaton model demonstrates cell motility increases fitness in solid tumors. The UCI Undergraduate Research Journal **12** (2009) 55-66.

ABSTRACT OF THE DISSERTATION

Mathematical and Computational Models of Virus Dynamics

By

Dustin Phan

Doctor of Philosophy in Ecology and Evolutionary Biology

University of California, Irvine, 2015

Professor Dominik Wodarz, Chair

Mathematical and computational models can provide unique insights into the dynamics of host-pathogen interactions *in vivo*. This dissertation explores these models in the context of multiple infection of cells and oncolytic virus therapy. In chapter one, we investigate the modeling of multiple infection using systems of ordinary differential equations, and demonstrate that the artificial truncation of the infection cascade required of numerical simulations can affect the distribution of multiply infection cells. As a result, models of multiple infection described by systems of differential equations require careful selection of parameter values and an appropriate cascade length to insure incorrect results are not observed. Chapter two explores this idea further in the context of two competing virus strains. Here, we find that cascade length can affect the equilibrium level of populations in numerical simulations. More specifically, competitive exclusion can be observed for shorter cascade lengths, whereas coexistence can be observed for longer cascade lengths. We also explore these models in a parameter regime in which cascade length does not affect the numerical simulations, and find that multiple infection can

promote coexistence if there is a degree of intracellular niche separation. We further find that multiple infection has a reduced ability to promote coexistence if virus spread is spatially restricted compared to a well-mixed system. Finally, chapter three presents an agent-based model of oncolytic virus therapy for the eradication of drug resistant cancer cells. Our results demonstrate that even if it is not possible to eradicate cancer with oncolytic viruses, it may be possible to eradicate the subpopulation of drug resistant cancer cells through apparent competition. Furthermore, we find that an increase in the infection efficiency of the virus can lead to higher levels of suppression of drug resistant cancer cells. This can increase the success rate of subsequent drug therapies in eradicating the cancer.

Chapter 1

Introduction

The study of biology as it relates to modern medicine has long been approached using observational and experimental methodologies. As science and technology has developed, advances in experimental methodologies have given us an increased understanding of biological systems, and how their interactions affect the functioning of cells and organisms under various circumstances. However, these experimental techniques are not without disadvantages. *In vitro* experimentation, for example, allows researchers to design controlled studies of specific systems in a simplified environment in order to gain insights into the interactions of specific biological components. Nevertheless, these insights do not easily translate to larger systems, and must be complemented with *in vivo* experimentation to observe the overall effects on whole organisms. Mathematical models provide a complementary approach to experimentation, and can provide useful insights into complex interactions. These insights, in turn, can provide the basis for the design of new experimental studies.

The use of mathematical modeling in the context of biology has long been used in the field of population ecology. In particular, research in the area of population dynamics investigates the complex interactions between different populations of organisms within a given environment. Thus, the concepts of population dynamics, coupled with mathematical modeling, are particularly suited to the study of virus infection dynamics *in vivo*. Nevertheless, such models must be based on empirical facts regarding the complex interactions between viruses and hosts, and any derived insights must be tested against experimental results. This dissertation explores the use of mathematical and computational models of host-pathogen interactions in a variety of contexts. In particular, we focus on the mathematical modeling of the multiple infection of cells by virus, and the computational modeling of oncolytic viruses for the eradication of drug resistant cancer cells.

1.1 The multiple infection of cells by viruses

Mathematical models of virus dynamics have been useful in complementing experimental research, giving rise to important insight into basic kinetics, disease processes, aspects of treatment, as well as the *in vivo* evolutionary dynamics of viruses [1-3]. Recently, the effect of multiple infection of cells by the same virus on infection dynamics has been explored, both experimentally and theoretically [4, 13-16]. Much of this work has been done in the context of human immunodeficiency virus (HIV), because multiple infection has been clearly documented to occur in this case.

While it has been observed *in vitro* that upon infection, the virus induces down modulation of its receptor on the surface of the infected cell, rendering the cell resistant to further infection events, it has become clear that multiple copies of HIV can infect the same cell [5-8]. Multiple infection of cells was demonstrated using reporter viruses labeled with different fluorescent colors [5, 7]. The occurrence of multiple infection in vivo is further supported by the finding that infected cells in the spleen from HIV-infected patients show on average 3-4 copies of integrated viral DNA [9]. While other studies have shown that in the blood most cells are infected with a single integrated copy of the virus [10,11], this is unlikely to represent a contradiction because processes that promote multiple infection of cells, such as direct synaptic transmission of the virus, are much less likely to occur in the blood than in tissue compartments. Evidence of viral recombination further substantiates the notion that multiple infection is a prevalent event in HIV infection [7, 9]. While documented less well, multiple infection of cells is likely to be also an important driving factor in other viral infections. For example, [4] showed that the initial dynamics of adenovirus spread in Ad-293 cells in vitro might be heavily influenced by the multiplicity of the virus in infected cells.

Multiple infection can have important consequences for the evolutionary dynamics of the virus in vivo [10, 18, 19]. In the context of HIV, the most commonly studied consequence is recombination between different viral genotypes that are packaged within the same virus particle. In addition, previous theoretical work has argued that competition dynamics between different virus strains can be influenced [20, 21]. In particular, previous models indicated that multiple infection of cells might allow the coexistence of different virus strains in settings where the absence of multiple infection would invariably lead to

competitive exclusion of one strain and the persistence of the fitter strain. This is similar in principle to epidemiological models that have demonstrated that multiple infection can allow the coexistence of different pathogens or pathogen strains that compete for the same host [22, 25, 26].

The exact assumptions and details of model construction, however, can influence the properties of the model [27, 28]. For the sake of analytical ease, relatively simple models have been used to study multiple infection of hosts or cells. In the simplest case, such models take into account three populations: hosts/cells infected with pathogen strain one or two only, and hosts/cells that are infected with both pathogen strains (Fig. 1.1). Such models have contributed to the notion that multiple infection promotes coexistence. It has been pointed out, however, that such simplified models can lead to questionable model properties, such as the existence of a defined stable equilibrium if the two pathogen strains are identical and thus competitively neutral [27, 28]. In the context of the in vivo dynamics of viral infections, such simplified models might be particularly unrealistic because it artificially limits the number of viruses that are allowed to occur in a cell. In reality, it is probably possible for many copies of a virus to infect a given cell, and this has to be taken into account explicitly.

It is important to note, however, that such pitfalls associated with artificially limiting the number of infections in a cell extends to more complex models as well. Models defined by systems of differential equations generally divide the total population of

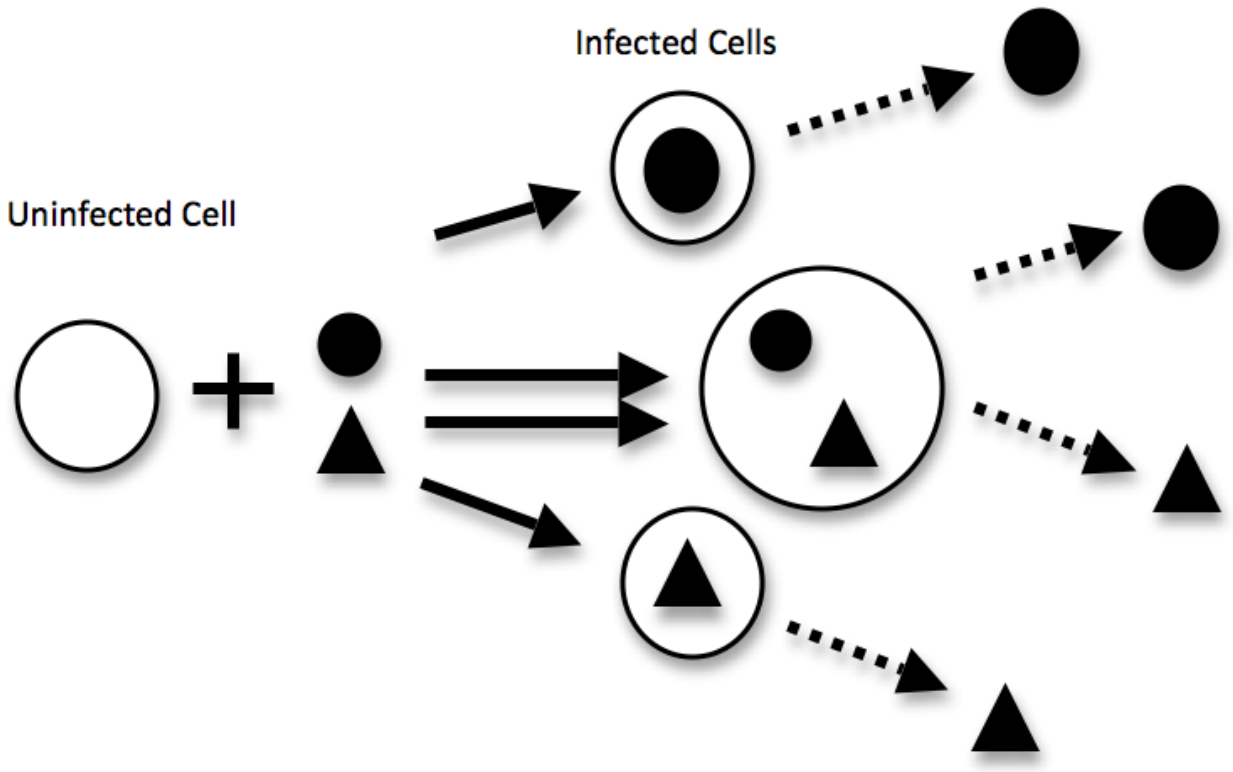

Figure 1.1. Schematic diagram illustrating the basic principles of models of multiple infection of cells by viruses. Assume the existence of two different virus strains. Cells infected by a single strain produce progeny of the type with which they were infected. Multiply infected cells may produce both virus types.

infected cells into subpopulations of cells infected by *i* viruses, and each subpopulation can in principal be infected to contain *i + 1* viruses. This is referred to as the "multiple infection cascade." In principle, this infection cascade can be infinite. In practical terms, however, the cascade must be cut artificially in order to study the model with numerical algorithms. As previously discussed, this can have an influence on the results in the context of multiple infection and virus competition.

Chapters two and three of this dissertation investigate the modeling of multiple infection of cells by viruses using ordinary differential equations in more detail. Specifically, chapter two investigates how artificially cutting the multiple infection cascade can affect the outcome in different parameter regions in the context of basic dynamics. Chapter three expands the multiple infection model to account for the competition between two virus strains. Here, competition for target cells, competition for intracellular resources, as well as the effects of spatial dynamics, are taken into consideration. Much of the analysis and discussion in these two chapters is in the context of HIV, because it is a relatively well-studied system. However, the insights gained here are general in nature, and can help lead to a better understanding of how model structure can influence the outcome in models that describe multiple infection of cells by viruses.

1.2 Oncolytic viruses for the eradication of drug resistant cancer cells

Cancer is a broad group of diseases involving the uncontrolled growth and proliferation of cells. This loss of growth regulation is the result of an accumulation of genetic mutations often beginning within a single cell. The genetic irregularities leading to this loss of growth regulation are the result of mutations within two basic types of genes: proto-oncogenes and tumor suppressor genes [61]. Under normal conditions, proto-oncogenes are responsible for the coding of proteins that regulate controlled cell growth and differentiation. Once activated by mutations, however, proto-oncogenes become

oncogenes, causing an increase in protein activity and a loss of growth regulation. Conversely, tumor suppressor genes code for proteins that have a dampening effect on the cell cycle. In addition, some are also responsible for promoting apoptosis, or programmed cell death. In healthy cells, any damaged or mutated DNA that cannot be repaired will cause an initiation of apoptosis. This is to prevent the proliferation of mutations and genetic irregularities. Thus, an accumulation of mutations leading to the activation of proto-oncogenes and the inactivation of tumor suppressor genes allows for the uncontrolled growth and proliferation of cells [61].

During the early stages of cancer development, localized solid tumors are typically removed by resective surgery. Once the cancer invades the lymph nodes or metastasizes and spreads to distant organs of the body, however, chemotherapy becomes the standard treatment method. The standard chemotherapy regimen involves the synergistic use of cytotoxic drugs to inhibit cell division. As a result, cells that are highly proliferative, a characteristic of cancer cells, are the ones that are affected most [34]. However, the cytotoxic properties of chemotherapy also extend to cells that have high proliferation rates under normal conditions. This includes cells in the bone marrow, the digestive track, and the hair follicles. Consequently, the most common side effects associated with chemotherapy are immunosuppression, inflammation of the digestive track, and hair loss [34, 35].

In an effort to minimize patient side effects and improve quality of life, the research and development of targeted cancer treatment methods has become increasingly popular. In particular, an increased understanding of altered molecular pathways in cancer has led

to the development of drugs that interfere with molecules required for the development of cancer [36-39]. One such example of a successful class of targeted cancer treatment drugs is tyrosine kinase inhibitors, such as Imatinib [42, 43]. In chronic myeloid leukemia, the tyrosine kinase enzyme BCR-Abl is continuously activated, leading to unregulated growth of the cell. In the presence of tyrosine kinase inhibitors, however, these cells stop growing and often die by apoptosis. In addition, the tyrosine kinase enzyme BCR-Abl is only present in cancer cells and not healthy cells, thus the drug is only cytotoxic to cancer. Despite the initial success of such small molecule inhibitors, drug resistance mutations often arise due to the genetic heterogeneity of many cancer populations [45-51].

In recent years, oncolytic viruses have been explored as an alternative targeted cancer treatment method. Oncolytic viruses selectively replicate in cancer cells, subsequently releasing viral progeny to infect neighboring cells and killing the host cell through lysis (Fig. 1.2) [54-59]. In principle, this leads to the eradication or control of the cancer. Tumor selectivity is made possible by a number of mechanisms. In some genetically engineered oncolytic viruses, for example, critical sections of the viral genome are placed under the control of tumor specific promoters. As a result, transcription occurs selectively in cancer cells. Many such promoters have been identified and studied for the treatment of cancers [62]. Other viruses may be engineered such that viral replication is blocked by certain genetic products present in healthy cells that are commonly missing in cancer cells, thereby allowing cancer selectivity [60, 62].

Despite promising results in clinical trials initially [52, 53], however, there have been few reports of sustained eradication or control of cancers using oncolytic viruses.

Even if the eradication of the cancer using oncolytic viruses cannot be achieved, however, it is theoretically possible to eradicate the subpopulation of drug resistant cancer cells through a simple population dynamics concept called 'apparent competition' [63, 64]. Even if two populations of species do not compete with one another directly, the population with the higher fitness can drive the other population extinct if they are infected by the same pathogen. In the context of chronic myeloid leukemia, certain drug resistant mutants have been shown to have a reduced growth rate, and are thus less fit than the drug sensitive strains [65]. Consequently, the oncolytic virus should be able to eradicate the subpopulation of drug resistant cancer cells, leaving only the drug sensitive population which can then be eradicated with drug therapy.

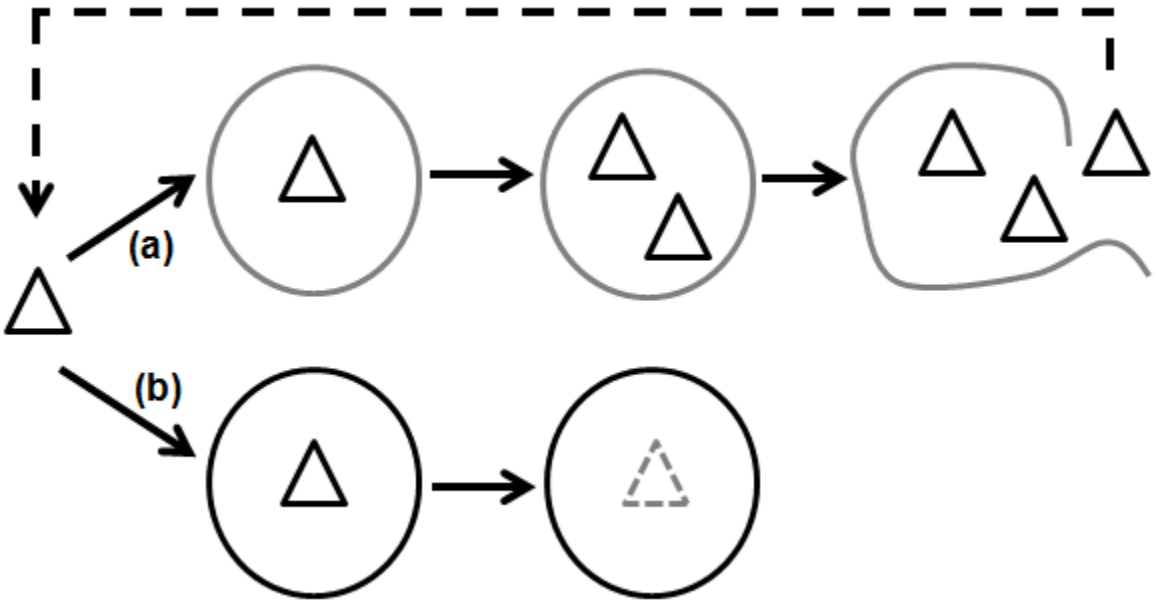

Figure 1.2. Schematic demonstrating the preferential replication and killing of oncolytic viruses in (a) cancer and (b) normal cells. If the oncolytic virus infects a cancer cell (a), it utilizes the host cell's machinery to replicate. Progeny virus kill the host cell by rupturing through, and proceed to infect nearby cancer cells. If the virus infects a normal cell (b), no viral replication takes place and the healthy cell remains undamaged.

Though many mathematical models describing the interactions of oncolytic viruses and cancer cells have been developed [67-72], [63] was the first to investigate these dynamics in the context apparent competition. These mathematical models, however, are based on systems of ordinary differential equations, and thus assume a perfect mixing mass action scenario. Nevertheless, while these assumptions may be valid for some non-solid tumors, the majority of tumors have intricate spatial structures where interactions are limited to local neighborhoods. In addition, models based on systems of ordinary differential equations are deterministic in nature, and lack the stochastic elements found in biological systems. An alternative method of modeling is the use of agent-based models.

Chapter four of this dissertation presents an agent-based model of oncolytic virus therapy. Here, the use of oncolytic viruses to eradicate the subpopulation of drug resistant cancer cells competition is investigated in a stochastic and spatially structured environment. These insights can provide the basis for more detailed explorations of targeted cancer treatment strategies involving oncolytic virus therapy.

Chapter 2

Modeling multiple infection of cells by virus

2.1 Introduction

Investigating the dynamics of virus spread through target cell populations has produced a better understanding of the principles underlying virus dynamics and evolution, and has provided insights into in vivo processes that contribute to the development of disease from a variety of human pathogens, such as human immunodeficiency virus (HIV), hepatitis B and C viruses (HBV and HCV). Mathematical models have played an important role in this respect [1–3]. A relatively underexplored area in virus dynamics is the multiple infection of cells, i.e. the simultaneous infection of a cell with more than one copy of a virus. This can occur in different infections. For example, adenoviruses are thought to infect cells with several viral copies, and interesting dynamics

have been observed that appear related to multiple infection and that warrant further investigation with mathematical models [4]. Some of the better documented data come from human immunodeficiency virus (HIV). A collection of in vitro and ex vivo studies clearly showed that more than one virus can enter the same cell [5–8]. For in vivo scenarios, patient data have been reported that showed an average of 3–4 proviruses per infected cell in the spleen [9]. Other studies, however, argued that the great majority of infected cells in HIV-infected patients in the blood and tissues are singly infected [10, 11]. This discrepancy might be due to the particular T cell subsets examined in the respective studies, although the reason is not understood. The occurrence of viral recombination in vivo, however, further indicates an important role of multiple infection, since recombination would otherwise not be possible [7, 9, 12].

Virus dynamics in the presence of multiple infection has been examined mathematically in a few studies. Basic dynamics were investigated with ordinary differential equations and integro-differential equations by Dixit and Perelson [13, 14], and subsequently investigated further in references [15,16], using ordinary differential equations and agent-based models. The effect of recombination, which requires multiple infection, has been modeled, e.g. [17–19]. Competition was also incorporated into multiple infection models [20, 21]. The ordinary differential equations models that have been reported are similar in structure compared to those in the field of epidemiology, where multiple pathogens are assumed to infect hosts [22–28].

Those models can be characterized by certain difficulties and pitfalls, especially when investigating simplified formulations in terms of ODEs. ODEs that describe multiple

infection generally divide the population of infected cells in subpopulations that are infected with one, two, three etc. viruses. We refer to this as the "multiple infection cascade". In principle, this cascade can be infinite. In practical terms, the number of cells infected with a multiplicity that lies above a certain threshold will be negligible, and thus the infection cascade can be truncated. It is, however, unclear how exactly the truncation of the cascade can affect the results. In the presence of competition, it has been shown that certain truncated and simplified model forms can lead to pathological outcomes, where the assumption of two identical (and thus competitively neutral) pathogens can lead to a unique equilibrium [27]. In this paper, we examine in more detail ODE modeling approaches to study the multiple infection of cells with viruses. Specifically, we investigate how the truncation of the multiple infection cascade can affect the outcome in different parameter regions in the context of basic dynamics.

2.2 Basic ODE models of multiple infection

Mathematical models of virus dynamics are often based on ordinary differential equations, and this approach has also been used to describe the infection of cells by multiple copies of the same virus (multiple infection). Denoting the population of susceptible cells by S, free virus by V, and the population of cells infected with i viruses by I_i, the model is given by (1).

This is an extension of basic virus dynamics models [1–3], and has been described first by Dixit and Perelson [13], with extensions published subsequently [2,3]. Susceptible

target cells are produced with a rate λ and die with a rate d. Infection of susceptible cells by virus occurs with a rate β, generating cells infected with a single copy of the virus. These cells can be infected by further virus particles with a rate β, generating cells infected with i copies of the virus. This process can continue until the end of the infection cascade, I_n, is reached. Cells in this population cannot be infected any further. Infected cell populations die with a rate a_i and produce virus with a rate k_i. Free virus decays with a rate u. In this formulation, the rate of virus production, k, and the rate of infected cell death, a, can depend on the multiplicity of infection, i, although it does not have to.

$$\begin{aligned}
\frac{dS}{dt} &= \lambda - dS - \beta SV \\
\frac{dI_1}{dt} &= \beta SV - a_1 I_1 - \beta I_1 V \\
\frac{dI_i}{dt} &= \beta I_{i-1} V - a_i I_i - \beta I_i V \\
&\ldots. \\
\frac{dI_n}{dt} &= \beta I_{n-1} V - a_n I_n \\
\frac{dV}{dt} &= k_i I_i - uV
\end{aligned} \tag{1}$$

In the simplest form, these parameters do not depend on the multiplicity of infection, as described by Dixit and Perelson [13]. In this case, virus production is determined predominantly by cellular factors, keeping the overall amount of virus produced constant and independent of the number of viruses in the cell. Alternatively, it is possible that the rate of virus production and the death rate of infected cells can increase to

a certain degree in multiply infected cells, a scenario considered in [16]. In models that have been applied to HIV infection, it has also been assumed that the ability of a cell to become infected can be lost over time, as a result of e.g. receptor down-modulation [13]. This will not be considered in the present context. For reference, parameters and their meaning are summarized in Table 2.1.

λ	Uninfected cell production rate
d	Uninfected cell death rate
β	Infection rate
a	Infected cell death rate
k	Free virus production rate
u	Free virus death rate
n	Infection cascade length

Table 2.1: Parameters for basic ODE model of multiple infection

One aspect we would like to explore here is the dependency of the dynamics on model structure. In particular, the ODE formulation requires an arbitrary end to the infection cascade, I_n. The larger the value of n, the more computationally expensive simulations of this system become. The value of n, however, can impact the dynamics that are observed in this model, and this will be investigated in the following sections. First, it will be assumed that virus parameters are independent of the infection multiplicity. Subsequently, we will assume that multiply infected cells produce more virus during their life-span than singly infected cells.

2.3 Virus parameters are independent of infection multiplicity

This system has been studied analytically before, and the reader is referred to these analyses for details [13,16]. If the basic reproductive ratio of the virus is greater than one, the virus and cell populations converge to an internal, stable equilibrium, which has been defined [13,16]. Here, we concentrate on the distribution of cells infected with different multiplicities. The most abundant infected cell population are singly infected cells, I_1, and the abundance of multiply infected cells, I_i, are successively lower (Fig. 2.1). The population size of the infected cell sub-populations decline exponentially with increasing multiplicities of infection (Fig. 2.2a), and the rate of this exponential decline is given by $\ln(\frac{\beta\lambda - ad}{\beta\lambda - ad - a^2})$ and hence depends on the parameters that determine the basic reproductive ratio of the virus. The faster the basic reproductive ratio of the virus, the slower the rate of decline. In other words, the singly infected cells become less dominant and the distribution becomes more even for faster viral replication kinetics. In the extreme case where the basic reproductive ratio of the virus is very large, all infected cell sub-populations are almost equally abundant.

If the decline of the successive infected cell sub-populations is relatively slow, the modeling approach discussed here can become difficult. If the length of the multiple infection cascade, n, is not sufficiently large, the majority of the infected cells will accumulate in the last member of the cascade, i.e. in I_n (Fig. 2.2b). This is clearly an unrealistic feature that can lead to artificial results (explored further below). For fast viral replication rates, it is possible to observe this behavior even if relatively large values of n are chosen, making it unlikely that the dynamics can be numerically studied in a realistic

way. Such parameter regimes are characterized by a very high average multiplicity of infection in the cells.

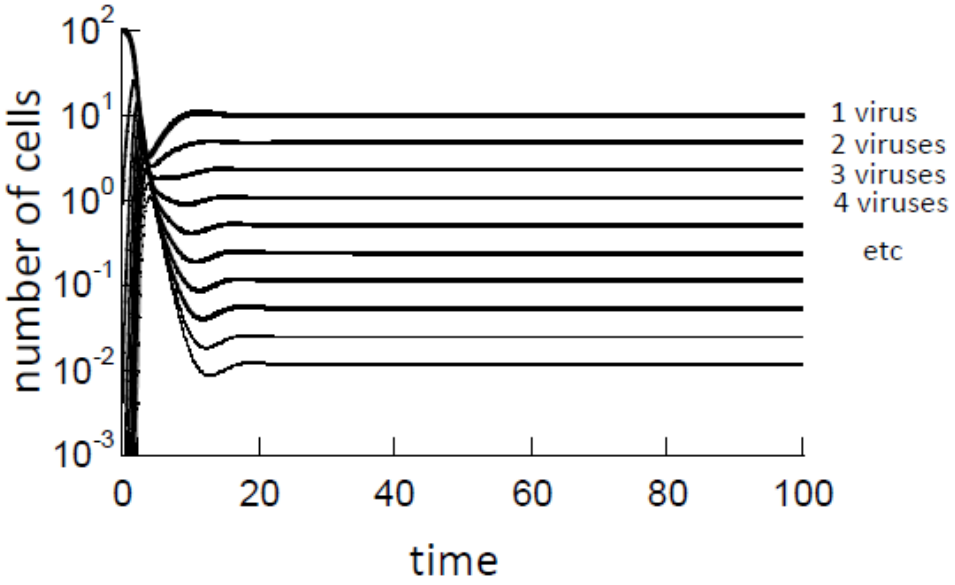

Figure 2.1. Distribution of the number of cells infected with I viruses, according to model (1) where the rate of virus production does not depend on infection multiplicity. Singly infected cells are most abundant, and the number of cells containing higher infection multiplicities is successively lower. Parameters were chosen as follows. λ=10; d=0.1; a=1; β=0.1; k=1; u=1; ε=0. Infection cascade length n = 100.

2.4 Virus parameters depend on infection multiplicity

Here, it will be assumed that the rate of viral replication increases in multiply infected cells. In this case, this also leads to an increase in the burst size of the infected cells (number of viruses produced during the life-span of the cell), which is given by k_i/a_i in the model [26]. For simplicity, it is assumed that only k_i is an increasing function of i, and that

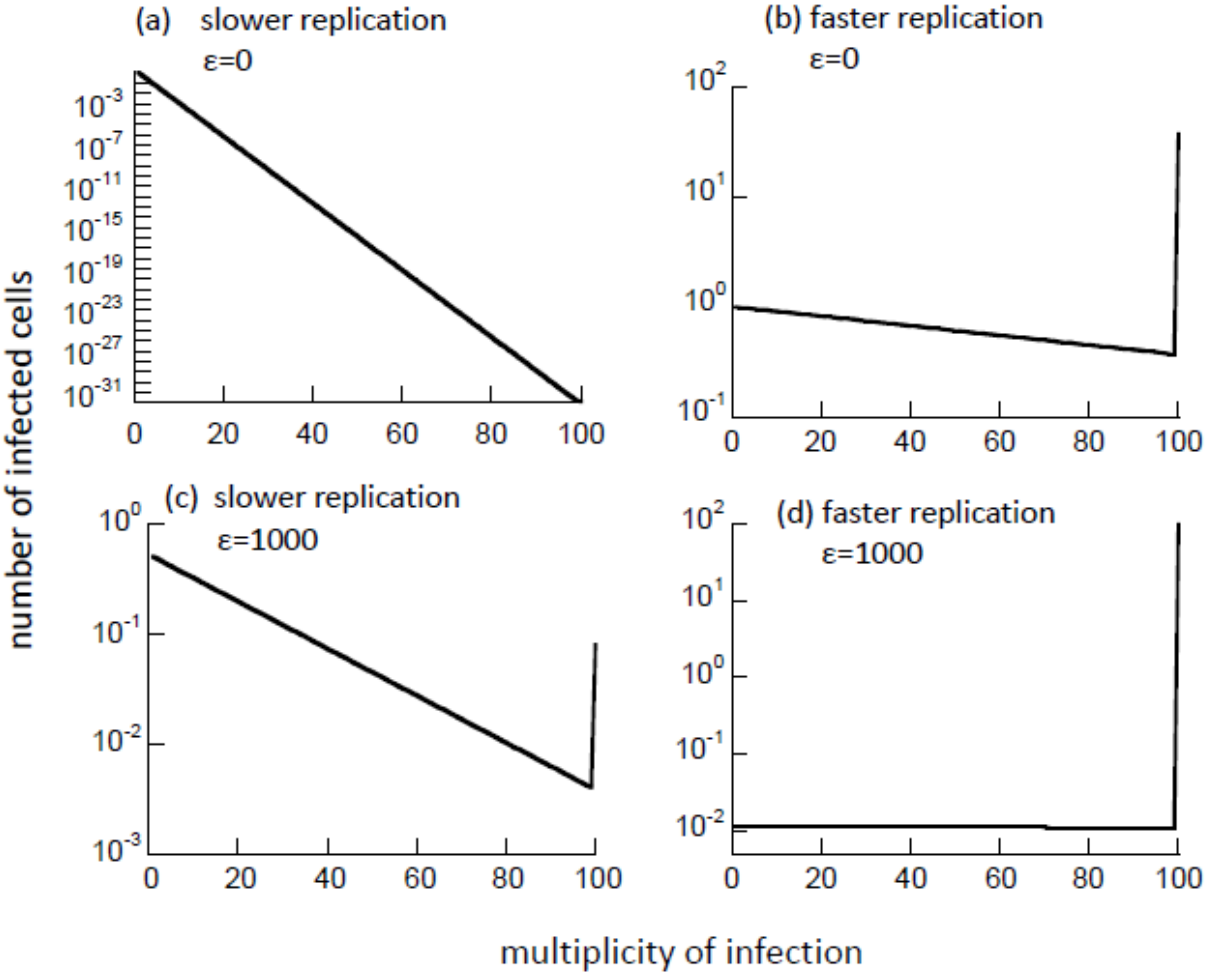

Figure 2.2. Equilibrium number of cells as a function of the infection multiplicity, according to model (1). The number of cells declines exponentially with the infection multiplicity. (a) If the rate of viral replication is relatively slow and does not increase with infection multiplicity, the numerical simulations reflect the expected exponential decline. (b) For faster viral replication rates, however, the equilibrium number of cells with increasing infection multiplicity declines much slower, and in numerical simulations, most infected cells accumulate at the end of the infection cascade, giving rise to artificial properties. (c, d) This effect is more pronounced if the rate of viral replication increases for higher infection multiplicities, ε>0. Base parameters were chosen as follows. λ=10; d=0.1; β=0.1; k=1; u=1. For (a) ε=0; a=2. For (b) ε=0; a=0.1. For (c) ε=1000; a=2. For (d) ε=1000; a=0.1. Infection cascade length n=100.

the death rate of infected cells remains independent of infection multiplicity. In particular, we will assume that the rate of virus production is given by $k\sum_{i=1}^{n}\frac{i(1+\varepsilon)}{i+\varepsilon}$. The overall rate of

virus production is a saturating function of the infection multiplicity. The parameter ε is the saturation constant. This parameter also appears in the numerator to avoid having to re-scale the parameter *k* if the value of ε is changed. For ε = 0, this expression reverts back to the previous model where the rate of virus production was independent of the infection multiplicity. For $\varepsilon \to \infty$, the rate of virus production increases linearly with the infection multiplicity. This extreme case, however, is most likely not realistic and will not be analyzed here.

We note that although a simplified scenario is considered in which only the rate of viral replication increases with the multiplicity of infection, the general results that we describe are not dependent on this simplification. The results hold as long as the burst size of infected cells (given by the rate of virus production divided by the infected cell death rate) increases with infection multiplicity. In reality, a higher viral replication rate can lead to a higher rate of infected cell death. As long as the increase in the death rate of infected cells is less than the increase in the viral replication rate at higher infection multiplicities, the burst size increases and our results hold. If the death rate of the infected cells increases more than the replication rate of the virus in multiply infected cells, the burst size of infected cells does not increase, which represents a different regime.

The properties of this type of model have been examined in a previous study [16], and can involve more complex dynamics. In particular, whether the infection is established or not can depend on the initial conditions, and hence, is not determined entirely by the basic reproductive ratio of the virus anymore. If an infection is established, the virus and cell populations again converge to a stable equilibrium, the properties of which have been

described before [16]. As in the previous model, the infected cell sub-populations at equilibrium are a declining function of the infection multiplicity, and the decline is again exponential. The exact rate of decline could not be calculated in this system. In contrast to the previous system (model one), however, there is a stronger tendency for the decline to be relatively slow, leading to a more even distribution of the infected cell sub-populations. The reason is that on average, the virus replicates faster as a result of the higher virus output from multiply infected cells. Hence, the average multiplicity of infection rises more as the replication kinetics of the virus are increased. Therefore, in this model it is easier to enter a parameter regime where most of the infected cells accumulate in the last element of the infection cascade, I_n, leading to difficulties for numerical simulations of this system (Fig. 2.2c and d).

2.5 Discussion and Conclusion

This chapter examined the use of ordinary differential equations for studying virus dynamics under the assumption that multiple viruses can infect the same cell. Here, we explored the basic dynamics where only one, homogeneous virus population exists. Such models have been studied before [13, 16], but we provided a more detailed account of how the length of the infection cascade can influence the results.

Previous studies that examined virus dynamics in the context of multiple infection often utilized simplified formulations in terms of systems of ordinary differential equations [13, 14, 16]. Nevertheless, such models can be characterized by certain pitfalls. Models that

describe multiple infection typically divide the population of infected cells into subpopulations of cells infected by one, two, three, etc. viruses. However, in practical terms, this infection cascade must be artificially truncated in order to solve the model numerically. Here, we examined this in a setting that involves a single, homogeneous virus population.

When virus parameters are independent of infection multiplicity, we observe that the most abundant infected cell population is singly infected cells, with the abundance of multiply infected cells successively decreasing. In general, the number of cells declines exponentially with the multiplicity of infection. However, how fast the numbers decline depends on the replication rate of the virus. Especially for larger viral replication rates, or for scenarios where viral replication increases in multiply infected cells, the number of cells harboring *i* viruses declines relatively slowly with the multiplicity of infection. In this case, most of the cells will accumulate in the last member of the infection cascade even for relatively long cascades, and this can influence the properties of numerical simulations. For such cases, the use of ODEs might be impractical, because very long infection cascades become computationally expensive.

This analysis is performed in the most general setting, without considering one specific infection. The aim of this chapter is to gain a better understanding of how model structure can influence outcome in models that describe the multiple infection of cells by viruses. This can form the basis for future work that applies this type of model to specific infections, which will require careful consideration of assumptions that are specific to the virus in question.

Chapter 3

The role of multiple infection on competition dynamics

3.1 Introduction

In recent years, many experimental and theoretical studies of host-pathogen interactions have investigated the dynamics of multiple infection of cells by viruses [1-3, 5-9]. Much of this work has been done in the context of HIV, where multiple infection been clearly documented and observed. In one study, *in situ* analysis of splenocytes from two HIV infected individuals demonstrated up to eight integrate integrated proviruses per infected cell, with an average of three to four integrated proviruses per infected cell [9]. Multiple infection has also been demonstrated using reporter viruses labeled with different fluorescent colors [5, 7]. In addition, analysis of genetic diversity found in individual cells and the prevalence of recombination *in vivo* further suggest the importance of multiple infection, since recombination would not be possible otherwise [9, 12].

Multiple infection can also have important evolutionary consequences *in vivo*. In particular, previous theoretical work has competition dynamics between different virus strains may be affects [20, 21]. Competition between different virus strains that infect the same target cell population has been studied with mathematical models, using approaches that are extensions of basic virus dynamics models that do not take into account multiple infection [1, 3]. In such scenarios, competitive exclusion is typically observed, where the virus strain with the higher basic reproductive ratio wins the competition. As expected from ecological theory, coexistence is observed in models that assume a degree of niche separation between the competing virus strains, such as the infection of different kinds of target cells [29–31].

Coinfection has been argued to be a mechanism that can promote coexistence [20–27], both in models that describe the spread of pathogens among hosts, and in models that describe the spread of viruses through cell populations. At the same time, it has been pointed out that model structure can be problematic in this respect [27]. Certain simplified models that are characterized by coexistence of competing strains have the unrealistic feature that a unique equilibrium is attained under the assumption that the two pathogen strains are competitively neutral, i.e. practically indistinguishable. Such models are not a good basis to explore the competition dynamics.

Previously, we explored a basic ODE modeling approach describing the multiple infection of cells with viruses. Specifically, we investigated how the truncation of the multiple infection cascade can affect the outcome in different parameter regions in the context of basic dynamics. We now expand the multiple infection model to investigate how

cascade length can affect the outcome of competition between two virus strains of different fitness. Then, using a parameter regime in which cascade length does not affect the results, we examine the effect of multiple infection on the outcome of competition. Here, we take into account both competition for target cells (as in standard virus competition models), and the competition for intracellular resources. Finally, we examine the effect of multiple infection on the outcome of competition when virus spread is spatially restricted.

3.2 ODE model of competition dynamics in the context of multiple infection

Here, model (1) of the previous section is extended to include two virus strains that compete for the same target cell population. Again, the model includes multiple infection cascades. In this case, cells can be infected with *i* copies of virus strain one and *j* copies of virus strain two, y_{ij}. The model is thus given by the system ordinary differential equations (2) as follows.

Cells susceptible to infection are produced by λ and die at rate *d.* Infection occurs at rate β_1 for strain one and β_2 for strain two, generating cells infected with a single copy of the respective strain. As in the previous chapter, infected cells can continue to incur additional infections until the end of the infection cascade is reached, here denoted by $I_{i+j=n.}$ Cells in this population cannot be infected any further. Infected cell populations die with a rate a_{ij}, and produce virus with rate k_1 and k_2 for strain one and strain two, respectively. Free virus decays at rate *u*. Again, the rate of virus production *k* and the rate of infected cell

death can depend on the infections incurred, though it does not have to. For reference, parameters and their meanings are summarized in Table 3.1.

$$
\begin{aligned}
\frac{dS}{dt} &= \lambda - dS - \beta_1 S V_1 - \beta_2 S V_2 \\
\frac{dI_{10}}{dt} &= \beta_1 S V_1 - a_{10} I_{10} - I_{10}(\beta_1 V_1 + \beta_2 V_2) \\
\frac{dI_{01}}{dt} &= \beta_2 S V_2 - a_{01} I_{01} - I_{01}(\beta_1 V_1 + \beta_2 V_2) \\
\frac{dI_{i,j}}{dt} &= \beta_1 I_{i-1,j} V_1 + \beta_2 I_{i,j-1} V_2 - a_{i,j} I_{i,j} - I_{i,j}(\beta_1 V_1 + \beta_2 V_2) \\
\frac{dI_{i+j=n}}{dt} &= \beta_1 I_{i-1,j} V_1 + \beta_2 I_{i,j-1} V_2 - a_{i,j} I_{i,j} \\
\frac{dV_1}{dt} &= k_1 \sum_{i=1}^{n} \sum_{j=1}^{n} \frac{(1+\varepsilon) i}{i + c_1 j + \varepsilon} I_{i,j} - u V_1 \\
\frac{dV_2}{dt} &= k_2 \sum_{i=1}^{n} \sum_{j=1}^{n} \frac{(1+\varepsilon) j}{c_2 i + j + \varepsilon} I_{i,j} - u V_2
\end{aligned}
\tag{2}
$$

λ	Uninfected cell production rate
d	Uninfected cell death rate
β	Infection rate of virus
a	Infected cell death rate
k	Free virus production rate of virus
u	Free virus death rate
ε	Saturation constant
c	Relative strength of interspecific competition
n	Infection cascade length

Table 3.1: Parameters for ODE model of multiple infection with competition dynamics.

The general model structure is the same as that explained in the previous chapter, except that we now track cells infected with two strains. The rate of virus production in infected cells merits further explanation. In a given cell, progeny virus of stain one is produced with a rate $\frac{k(1+\varepsilon)i}{i+c_1 j+\varepsilon}$. This captures competition between the virus strains within a cell. Different viruses or virus strains are likely to use common resources within the cell, thus introducing competition for cellular products. Hence, the rate of virus production of strain one is negatively impacted by both the presence of further viruses of the same strain (intraspecific competition, i), and by viruses of the second strain (interspecific competition, j). The relative strength of interspecific competition is captured in the parameter c_1. If $c_1 = 1$, the negative impact of strain two on strain one is identical to the negative impact of additional strain 1 genomes on themselves. If $c_1 < 1$, the degree of interspecific competition is reduced. That is, strain two viruses have less of an impact on strain one than strain one has upon itself. In the extreme case where $c_1 = 0$, the two virus strains replicate independently within the cell and there is no competition for intracellular resources. If $c_1 > 1$, a strain two virus has a stronger impact on strain one than strain one viruses have upon themselves. This can be interpreted as direct inhibitory effects. In the extreme case for large values of c_1, strain one practically does not produce offspring in cells that are coinfected with both strains. This is a "winner takes it all" situation, where strain two is the winner. The same arguments hold for the production rate of virus strain two, where the parameter c_2 describes the degree of inhibition of strain two by the presence of strain one.

We need to add some more clarifying remarks about the case where $c_{1,2} < 1$. If $c_{1,2} = 1$, the interpretation is that these are two strains of the same virus. In the opposite extreme,

$c_{1,2}$ = 0 means that they are two separate viruses that infect the same cells. Complete lack of resource sharing means that they replicate by completely separate mechanisms. For 0 < $c_{1,2}$ < 1, the situation is intermediate. When we analyzed models for a single virus population, we distinguished between two scenarios: (i) Viral parameters are independent of the infection multiplicity. In this case, the burst size of the infected cell did not depend on the infection multiplicity either. (ii) Viral parameters, and thus the burst size of the infected cells, do depend on infection multiplicity. In the context of two competing viruses, scenario (i) is a little more complex. This is best illustrated for $c_{1,2}$ = 0. Even if viral parameters are independent of how many copies of this virus reside in the cell, the total burst size of a cell that contains both virus of type one and virus of type two is higher compared to the burst size of a cell that contains only one virus type. Hence, in this case there is no clear correlation between whether viral parameters do or do not depend on infection multiplicity and the total burst size of infected cells. Similar considerations apply if 0 < $c_{1,2}$ < 1. This should be kept in mind in the following sections.

To summarize, this model contains two layers of competition: competition for the common pool of target cells (as assumed in standard virus dynamics models without coinfection), and intracellular competition for resources that are required for viral replication. The balance of these two forces determines the outcome of the competition, which is investigated below. Two virus strains with the following characteristics will be considered. Strain one will be the "superior" strain, characterized by a faster replication rate than the "inferior" strain two (i.e. $k_1 > k_2$). This makes strain one the better competitor for the target cell pool. This is analogous to a competitive advantage in simpler models that do not allow for multiple infection, and thus allows us to compare how multiple infection

modulates the outcome of this competition. For simplicity, all other parameters are assumed to be identical for the two virus strains. In our analysis, we will first assume that multiple infection does not influence viral parameters. Subsequently, this will be examined assuming that the rate of virus replication increases with the multiplicity of infection.

3.3 Virus parameters are independent of infection multiplicity

We only consider parameter regions in which each virus strain can persist in isolation. We find that both competitive exclusion and coexistence are possible, depending on the model parameters (Fig. 3.1). Coexistence only occurs if $c < 1$. That is, on an intracellular level, a degree of niche separation is required. In other words, the two virus types/virus strains need to utilize the intra-cellular resources in a somewhat different manner. Further, the replication kinetics of the viruses plays an important role. Fig. 3.2 shows the outcome of competition as the virus spread parameters, as well as the parameter c are varied. The rate of virus spread is determined by a variety of parameters. In Fig. 3.2a, we vary the death rate of infected cells, a, and in Fig. 3.2b, we vary infection rate of the viruses, β. A higher infection rate and a lower death rate of infected cells increase the rate of virus spread. We observe that extinction of the inferior competitor is promoted by slower virus spread and by high values of c.

For slower virus spread, the equilibrium number of uninfected cells is relatively high, and the equilibrium number of infected cells is relatively low. Therefore, new infections likely result in singly infected cells and multiple infection is not a very important

force driving the dynamics. Hence, competition for target cells is the most important determinant of the dynamics, and the properties of the model are similar to those of a model that does not take into account multiple infection. Consequently, competitive exclusion occurs. For faster virus spread, on the other hand, many coinfected cells are generated and the competition for target cells is reduced. Now, intracellular competition becomes an important driving force of the dynamics, and coexistence occurs as long as there is sufficient resource separation between the two virus strains within the cells (value of c below a threshold). How large the coexistence parameter regime is depends on the fitness cost of the inferior virus. In Fig. 3.2a and b, a 5% fitness cost was assumed and coexistence was observed for values of c up to 0.9 (where $c = 1$ means complete resource overlap). For higher fitness costs, the coexistence regime is reduced and lower values of c are necessary (Fig. 3.2c, illustrated for the case where the parameter a was varied, c.f. Fig. 3.2a).

So far, we have not examined the assumption of $c_{1,2} > 1$, i.e. when there is active interference among the viruses, with the extreme assumption being that the winner takes it all. In this case, the outcome of competition can depend on the initial conditions. A higher initial abundance of one virus strain relative to the other promotes the persistence of this virus strain and the exclusion of the competitor. Thus, if the relative initial abundance of the inferior strain is sufficiently large, it can win the competition. The higher the fitness disadvantage of the inferior strain, the higher its relative initial abundance needs to be for it to win. These patterns have been explored with computer simulations, although they are not graphically shown here. This dependence on initial conditions is similar that seen in standard Lotka–Volterra competition equations [32].

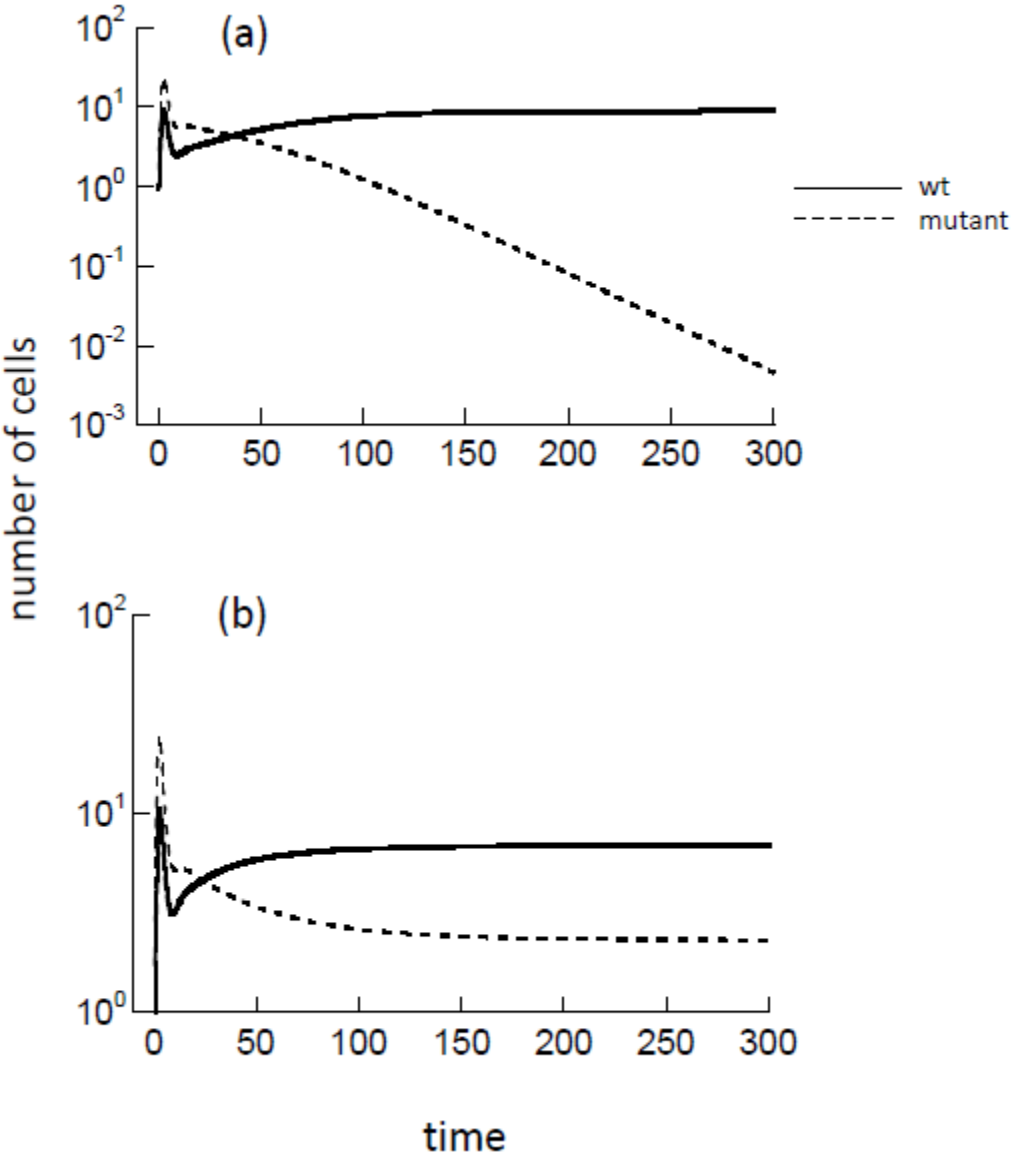

Figure 3.1. Outcomes of the competition model (2). (a) Competitive exclusion. (b) Coexistence. Parameters were chosen as follows. $\lambda = 10$; $d = 0.1$; $\beta = 0.1$; $k_1 = 1$; $k_2 = 0.95$; $u = 1$; $\varepsilon = 0$. For (a) $c = 1$, for (b) $c = 0.7$. Note that the only difference between the two strains was assumed to lie in the rate of virus production, k. Infection cascade length $n = 100$.

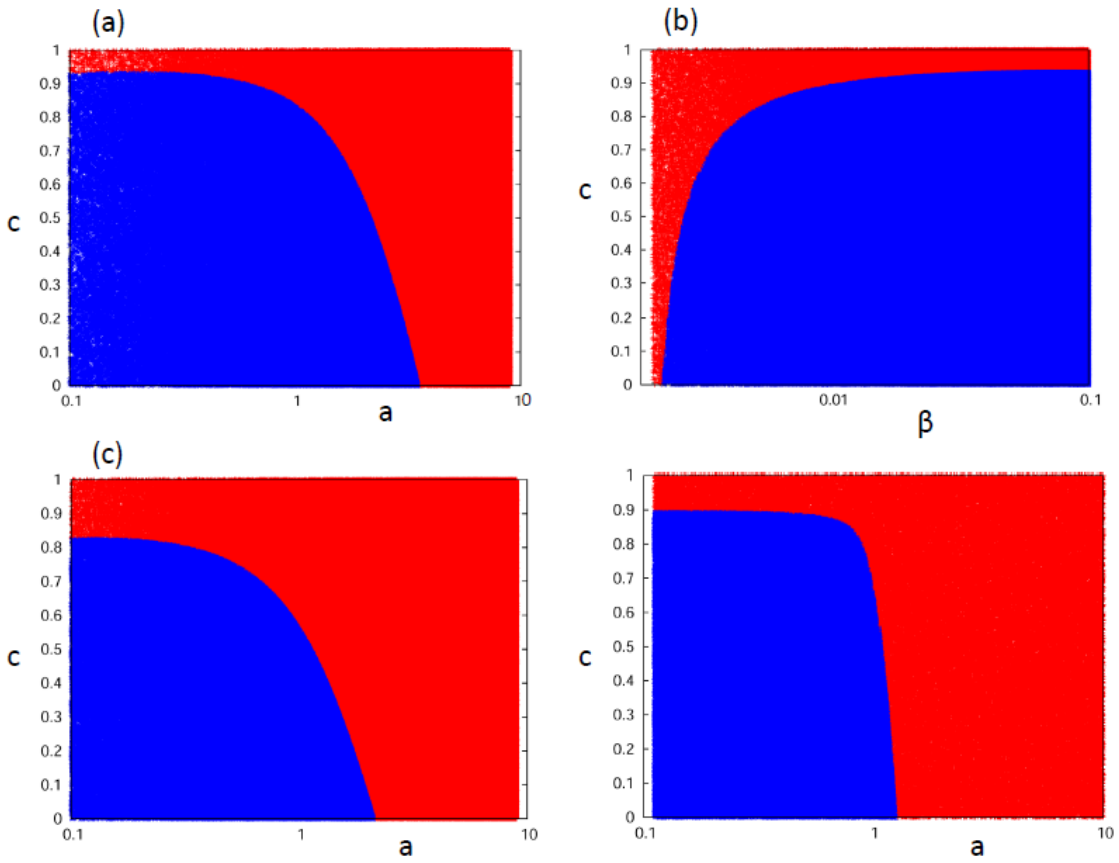

Figure 3.2. Outcome of competition in model (2), depending on parameters that determine the rate of virus spread, and the parameter *c*, which describes the relative strength of intracellular competition among the two virus strains. Blue indicates coexistence, while red indicates exclusion of the inferior mutant by the wild-type. Results are based on numerical simulations. (a) Effect of the death rate of infected cells, assuming that the mutant has a 5% fitness cost compared to the wild-type virus. The higher the death rate of infected cells, the slower the spread of the virus, and the more difficult it is to observe coexistence. That is, for higher values of *a*, coexistence requires a lower value of *c*, i.e. more intracellular niche separation. If the value of a lies above a threshold, coexistence is impossible. (b) Effect of the rate of infection, assuming a 5% fitness cost. The lower the rate of infection, the more difficult it is to observe coexistence. (c) Same as (a), but with a 15% fitness cost, which reduces the coexistence regime. (d) Same as (a), but assuming increased viral output in multiply infected cells. Now, the coexistence regime is larger. Parameters were chosen as follows. $\lambda = 10$; $d = 0.1$; $a = 0.2$; $\beta = 0.1$; $k_1 = 1$; $u = 1$. For (a, b) $k_2 = 0.95$; $\varepsilon = 0$. For (c) $k_2 = 0.85$; $\varepsilon = 0$. For (d) $k_1 = 0.95$; $\varepsilon = 50$. Infection cascade length $n = 100$. Larger infection cascade lengths (up to $n = 500$) were also explored and did not change the results plotted here. These simulations were computationally much more costly, were not run to include as many data points, and are hence not shown.

3.4 Virus parameters depend on infection multiplicity

The above analysis was repeated assuming increased viral replication rates in multiply infected cells. The corresponding results are shown in Fig. 3.2d for parameter values that correspond to those used in the last section (compare to Fig. 3.2a). We observe that results are qualitatively similar, but that an increased virus replication rate in multiply infected cells leads to a smaller parameter regime in which coexistence is observed. Faster viral replication in multiply infected cells essentially increases the fitness discrepancy between the two viruses. The superior virus will multiply infect more cells than the inferior virus. Hence it will enjoy the resulting faster replication kinetics in a larger number of cells than the inferior virus. This in turn leads to a more pronounced fitness advantage, explaining the numerical observations.

3.5 Effect of the infection cascade length

The previous chapter examined basic multiple infection dynamics assuming a single virus population. We found that the length of the multiple infection cascade, n, can have an influence on the dynamics especially if the basic reproductive ratio of the virus is relatively large and the average multiplicity of infection is relatively large. In this case it is possible that most infected cells accumulate at the end of the infection cascade, i.e. in I_n. For the competition model, it was assumed that the end of the cascade was reached when $i + j = n$. Because cells at the end of the cascade cannot be infected anymore, the opportunity for multiple infection to occur is reduced, and this can affect the outcome of competition. This

is demonstrated in Fig. 3.3. With a relatively large cascade length of n = 100, coexistence is observed. With the shortest cascade length (n = 2), competitive exclusion occurs. With a cascade length of n = 5, the outcome is again coexistence, but the equilibrium levels of the virus populations are different compared to n = 100. This shows that the assumed cascade length can have a profound influence not only on the observed dynamics, but also on the qualitative outcome of the interactions between the viruses. Therefore, special attention has to be given to the cascade length when studying such dynamics, ensuring that an increase in n does not lead to different dynamics. This was done in the previous section which analyzed the competition outcomes.

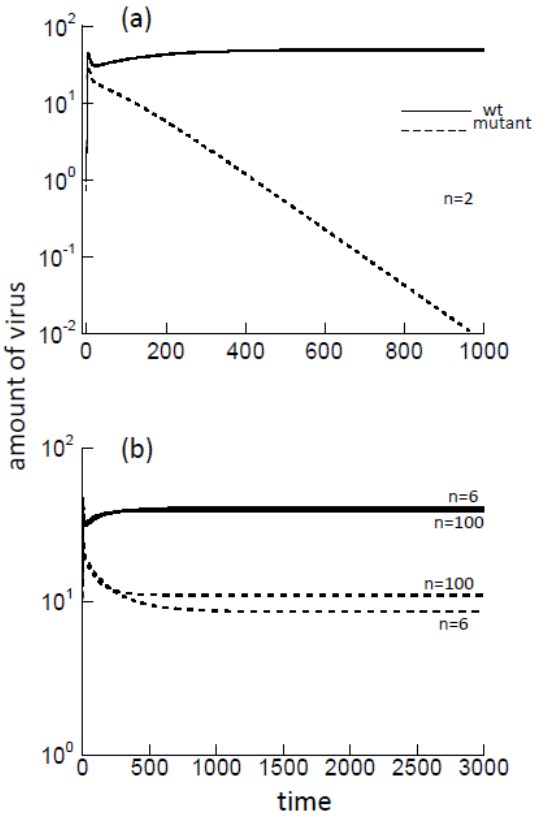

Figure 3.3. Dependence of the competition outcome in model (2) on the length of the infection cascade, n. (a) For n = 2, numerical simulations lead to competitive exclusion. (b) For higher values of n, coexistence is observed. However, the equilibrium population values to which the simulations

converge can depend on the exact length of the infection cascade. Thus, when studying the competition dynamics with this model, it is important to make sure that parameter regions are considered where the length of the infection cascade does not influence outcome or equilibrium values in numerical simulations. Parameters were chosen as follows. $\lambda = 10$; $d = 0.1$; $a = 0.2$; $\beta = 0.1$; $k_1 = 1$; $k_2 = 0.95$; u = 1; $c = 0.9$, $\varepsilon = 0$. Cascade lengths are indicated in the figure.

3.6. Effect of space

The previous analysis assumed perfect mixing of populations, i.e. mass action. Here, we consider a spatially explicit model in order to examine the effect of spatial restriction on the outcome of competition. This is done with a stochastic, agent-based model that tracks the fate of individual cells.

This modeling approach also eliminates the problem of infection cascades explored in the previous section, because it tracks individual cells and their multiplicity of infection. The model assumes a two-dimensional grid of size N x N, and is described as follows. Each spot in the grid can be empty, contain an uninfected cell, or contain an infected cell that is characterized by its multiplicity of infection. At each time step, N^2 spots of the grid are randomly sampled. If the sampled spot is empty, an uninfected cell can be produced with a probability L. If the sampled spot contains an uninfected cell, it can die with a probability D. If the sampled spot contains an infected cell, the following actions can occur. The cell can die with a probability A. Alternatively, the cell can attempt to pass on the infection to another cell with a probability B. In this case, a cell within a given neighborhood is randomly chosen as a target for infection. If the chosen spot is empty, no infection occurs. If the chosen spot contains an uninfected cell, it becomes infected with one virus. If the

chosen spot contains an already infected cell with a given multiplicity, another virus is added to this cell. A description of the parameters of this model can be found in Table 3.2.

The radius around the source cell from which a target cell is chosen can be varied. At one extreme, the target cell can be chosen from all cells in the system, and this corresponds to mass action, also described by the above ODEs. At the other extreme, the target cell is chosen from the eight nearest neighboring cells, and this corresponds to the most stringent degree of spatial restriction. We will compare the dynamics assuming nearest neighbor interactions and mass action.

N	Grid size N x N
L	Probability of producing uninfected cell
D	Probability of uninfected cell death
A	Probability of infected cell death
B	Probability of infecting another cell
c	Degree of intracellular competition

Table 3.2: Parameters for agent based model of multiple infection with spatial dynamics.

As before, two virus strains are assumed to be present. Hence, a cell can be infected with i copies of virus one and j copies of virus two. The rate of virus production is determined as follows for each strain present in the cell. For each copy of the virus a target spot is randomly chosen. If the chosen spot contains a susceptible cell, this copy gets

passed on with probability $\frac{1+\varepsilon}{i+c_1 j+e}$ for strain one, and $\frac{1+\varepsilon}{c_2 i+j+\varepsilon}$ for strain two. This corresponds to the same assumptions that were made for the ODEs in the previous sections, and captures the intracellular competition between the virus strains in the same way. As before, if ε =0, virus parameters do not depend on the multiplicity of this virus in the cell. If ε >0, the rate of virus replication increases if multiple copies of this virus infect the cell. For simplicity, we will concentrate our analysis on the ε =0 scenario for the spatial analysis.

In general, for the nearest neighbor scenario, the same types of outcomes are observed as in the mass-action scenario, and the determinants of the outcome are qualitatively identical. This was obtained by extensive numerical simulations of the model (Figure 3.4a). We were interested in whether the parameter regime under which extinction occurs was smaller or larger for the nearest neighbor situation compared to mass action. Hence, we compared the two scenarios in the following way. We determined the outcome as a function of the infection rate of the virus, *B*, and the competition parameter *c* (Figure 3.4a). We then superimposed the extinction parameter regions for the spatial and the non-spatial scenarios in order to compare which one is larger. For this, we note that the spatial model has a higher threshold value of *B* required to sustain the infection than the mass action model. Thus, to properly compare the extinction regimes for the two scenarios, we subtracted the difference in the threshold values from the *B*-parameter in the spatial simulations.

The results are shown in Figure 3.4a. We observe that the extinction regime is larger in the spatial compared to the mass action scenario. In other words, competitive exclusion

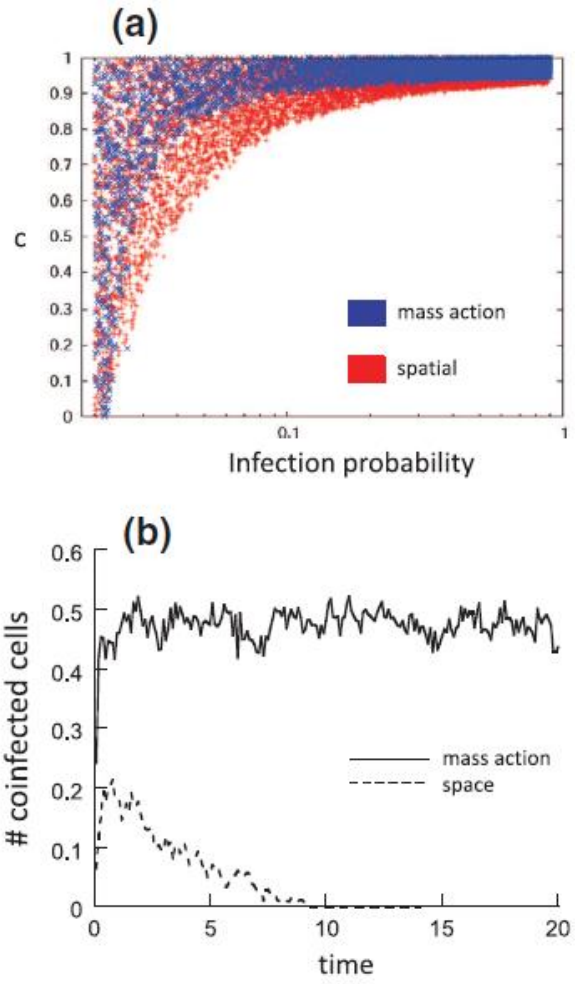

Figure 3.4. (a) Competition in spatial (nearest neighbor) versus non-spatial (mass-action) settings, using the agent-based model described in the text. Only the extinction parameter region is plotted, both for the spatial (red) and mass-action (blue) settings, depending on the infection probability B and the intracellular competition parameter c. Because in stochastic simulations, population extinction will occur if the simulation runs for a sufficiently long period of time, the outcome of competition was determined as follows. Initial conditions were used in which spontaneous extinction of either virus in isolation was very unlikely. One hundred infected cells of each type were seeded randomly across the grid. If the inferior strain went extinct before a time threshold, the outcome was recorded as competitive exclusion. Otherwise, the outcome was recorded as coexistence. The time threshold was chosen such that the outcome did not change if the duration of the simulation was increased further. As mentioned in the text, the spatial and the non-spatial simulations have different infection rate thresholds for establishment of infection. To directly compare the size of the extinction regimes in the two settings, we subtracted the difference in the threshold values from the infection probability parameter in the spatial simulations. Parameters were chosen as follows. L=0.8; D=0.01; A=0.02; ε=0. The grids size was 50 x 50. (b) Reason for the

larger extinction region in the spatial simulation. In the spatial setting, fewer cells are generated that contain both virus strains than in the mass-action setting, accounting for the larger extinction regime. Parameters were chosen as follows. L=0.8; D=0.01; A=0.02; B=0.0623; c=0.73; ε=0. The grids size was 50 x 50.

is promoted by nearest neighbor interactions. The reason for this result is shown in Figure 3.4b. For the nearest neighbor model, the two virus strains are less likely to meet in the same infected cell. Although multiple infection readily occurs, cells are typically infected with multiple copies of the same virus. Thus, Figure 3.4b shows that the fraction of cells infected with both virus strains remains significantly lower in the spatial setting compared to the mass action setting. Because the reason for the coexistence is the occurrence of coinfection with both strains, the coexistence regime is reduced, and extinction occurs over a wider parameter regime.

3.7 Discussion and Conclusion

These models were then expanded to study competition dynamics. Previous work has shown that inappropriate model simplification can give rise to pathological results, such as the presence of a unique coexistence equilibrium if two strains are competitively neutral [27]. Here, we show that even if the model is formulated in a way such that this effect is not observed, the outcome of competition can be influenced by the length of the infection cascade. For example, for identical model parameters, competitive exclusion can be observed for shorter infection cascades, while coexistence is observed for longer cascades. There can also be more subtle effects, where the equilibrium population levels

that are observed in numerical simulations can vary, depending on the length of the infection cascade. Therefore, when studying such competition dynamics with ODEs, it is important to make sure that a parameter regime is explored in which an increase in the length of the infection cascade does not change the results of numerical simulations.

In this regime, we investigated whether multiple infection can promote the coexistence of two virus stains with different fitness. In equivalent models that do not take into account multiple infection, competitive exclusion tends to be the only outcome [1]. With multiple infection, however, we found that coexistence can occur in the models studied here, but we need to distinguish two levels of competition: competition for target cells, as in previous virus dynamics models that do not take into account multiple infection; and competition for intracellular factors. If the two viruses / virus strains in question use the exact same intracellular resources, i.e. if their intracellular niches completely overlap, then multiple infection cannot lead to the coexistence of the strains. The faster growing strain will win and exclude the slower growing strain. If, on the other hand, there is a degree of niche separation within cells, then multiple infection can allow the coexistence of the different viruses, consistent with general ecological theory [32]. The crucial factor is not the multiple infection in general, but the simultaneous infection of cells by the two different viruses. If a sufficient number of cells harboring both viruses is generated, then coexistence becomes possible. This in turn can be influenced by assumptions about virus spread. We showed that spatially restricted virus spread leads to lower numbers of cells carrying both viruses because spatial restriction promotes multiple infection of cells with the same virus type rather than the coinfection with both types. Hence, multiple infection promotes coexistence of strains to a lesser degree in a spatial setting compared to a well-

mixed system. In general, this analysis indicates that related strains of the same virus are unlikely to coexist in the context of multiple infection, but that multiple infection can promote coexistence of different viruses with separate replication mechanisms that infect the same cells.

Our analysis provides important new insights into the properties of models that describe the multiple infection of cells by viruses. This can form the basis for building such modeling approaches for specific infections, where particular biological realities need to be taken into account for accurate descriptions. An interesting case study to explore would be adenoviruses, where multiple infection is thought to readily occur and where multiple infection is thought to allow the virus to replicate at a faster rate. In a set of experiments a culture of 293 cells, arranged in a 2-dimensional monolayer with agar layover, was infected with an engineered fluorescent adenovirus at very low multiplicities of infection [4]. This allowed the very early spread of the infection from a single infected cell to be monitored over time. It was found that once at least three infected cells were generated, virus spread became significantly faster and the virus population never went extinct anymore. This was inconsistent with the expected extinction probabilities calculated from parameters that were estimated from singly infected cells. Because in the 2D monolayer culture, spread of the virus to nearest neighbors was ensured by agar layover, multiply infected cells became readily generated as soon as the virus had spread to only a few cells. This in turns accelerated the rate of viral replication, accounting for the experimental observations. A better understanding of those growth dynamics, and an investigation of competition dynamics between different virus strains in such a setting, would be important to gain further insights into the spread of adenoviruses, which would also be relevant for human

health. This will require multiple infection models that are based on the ones discussed here and that also take into account spatial aspects. Our work provides guidelines for such an analysis. As summarized at the beginning of this article, multiple infection has also been observed with HIV, and a variety interesting questions remain to be explored in this respect. The relevance of multiple infection in vivo, however, has been debated, and there is the additional complication that multiple infection is promoted by direct cell-to-cell transmission through virological synapses [8], which requires different modeling approaches [33].

Chapter 4

A computational model of oncolytic viruses for the eradication of drug resistant cancer cells

4.1 Introduction

Current cancer treatment strategies typically involve the synergistic use of drugs, along with radiation therapy and surgery, in an effort to bring cancer growth and development under control. The cytotoxic properties of chemotherapeutic drugs, however, are general in nature, and thus affect cells with high division rates under normal circumstances, often leading to signifcant side effects [34, 35]. In recent years, increased understanding of altered molecular pathways in cancer cells has lead to the development of small-molecule inhibitors as a form of targeted therapy [36-39]. Since cancer cells are

selectively targeted, the degree of side effects is significantly reduced compared to conventional chemotherapy. One such example of successful small-molecule inhibitor drugs is Imatinib, which is used in the treatment of multiple cancers, most notably chronic myeloid leukemia (CML) [40-44]. Cancers, however, typically consist of mixed, genetically distinct populations of cells, many of which are are drug resistant, and thus, therapy resistant, particularly at more advanced stages of cancer [45-51].

Oncolytic viruses are an alternative targeted cancer treatment strategy that has shown promising results in clinical trials [52, 53]. These viruses, either naturally occuring or genetically engineered, preferentialy infect and kill cancer cells [54-59]. In principle, oncolytic viruses spread through the cancer population, replicate, and lyse the infected cells, leading to eradication or control of the cancer. The selective properties are possible because viral replication is blocked by certain genetic products present in healthy cells that are commonly missing in cancer cells. For example, the H-101 adenovirus developed by Shanghai Sunway Biotech has been engineered to remove a viral defense mechanism that interacts with a normal *p53* tumor supressor gene, which is often dysregulated in cancer cells [60, 61]. Despite promising initial results, however, sustained and reliable treatment success has yet to be reported [62].

Thus far, the goal of oncolytic virus therapy has been to eradicate the cancer. It has been previously reported, however, that even if eradication of the cancer cannot be achieved, it is theoretically possible to eliminate the subpopulation of drug resistant mutants [63]. In principle, the cancer is pretreated with oncolytic viruses, thereby driving the drug resistant mutant population to extinction. This leaves the subpopopulation of

cancer cells that is drug sensitive, which can be subsequently controlled by conventional chemotherapy or small-molecule inhibitor drugs such as Imatinib.

The rationale for this treatment strategy is a concept derived from population dynamics known as 'apparent competition,' the indirect competition of two species by a common predator [64]. In the context of oncolytic viruses, even if two populations of cells do not directly compete with one another, the fitter strain may be able to competitively exclude the less fit strain if they are infected by the same virus. For example, if the proliferation rate of the drug sensitive cancer cells is higher than the proliferation rate of the drug resistant cancer cells, than the drug resistant cancer cells may be driven to extinction through an oncolytic virus. This is made possible because drug resistant mutants incur a replicative fitness cost in the form of reduced growth rates, and are thus less fit than drug sensitive cells [65]. While replicative fitness costs have been observed in infectious diseases such as human immunodeficiency virus (HIV), this remains to be investigated in more detail in the context of cancer [66].

Many mathematical models of oncolytic virus therapy have utilized ordinary differential equations that describe the interactions between the replicating virus and growing populations of tumor cells [67-72]. In particular, [63] explores the use of oncolytic viruses for the eradication of drug resistant cancer cells in the context of apparent competition. Nevertheless, one of the assumptions of such modeling techniques is the perfect mixing of virus and cancer cells in a mass action environment. The majority of tumors, however, have intricate spatial structures where cells and virus do not necessarily mix, and interactions are limited to localized neighborhoods. Furthermore, these systems

are deterministic, and lack the stochasticity present in nature. An alternative modeling approach is the use of agent based models, where each cell is represented as an autonomous agent interacting with other cells based on probabilistic rules. This chapter utilizes an agent based model to explore the idea of using oncolytic viruses to selectively eradicate drug resistant cancer cells. Agent based models allow us to explore cell competition dynamics and oncolytic virus infection in a stochastic spatial environment. Insights derived from this model can provide the basis for more detailed explorations, and can guide future experimental design.

4.2 Agent-based model of oncolytic virus infection

Tumors are often characterized by spatial structures that cannot be captured by ordinary differential equations. In order to study the interactions between oncolytic viruses and cancerous cells, we utilize a model that takes into account the spatial distribution of the uninfected and infected cells. Here, we use the agent-based modeling technique. Each spot on a grid is represented by an "agent" or cell, which then interacts with other cells according to stochastic interaction rules based on biological processes. Given the state of the simulation space at time *t,* the set of stochastic interaction rules is applied to each grid point, giving rise to the state of the system at time $t+1$.

Our agent based model considers a two-dimensional grid that contains $N \times N$ grid points. Each grid point is characterized by one of five states: empty, occupied by an uninfected wild-type cell, occupied by an uninfected mutant cell, occupied by an infected

wild-type cell, or occupied by an infected mutant cell. At each time step, the grid is randomly sampled N^2 times. Depending on its state, the chosen spot interacts with its environment based on the following rules. If the chosen grid point is an uninfected cell of any type, it dies with probability D, and thus persists with probability $1-D$. Uninfected wild-type cells that undergo treatment have a probability of death W, where $W > D$. Cell death will result in an empty grid point into which other uninfected cells may be produced. Uninfected wild-type cells may proliferate with a probability of P, and a destination spot is randomly chosen for the offspring from one of the eight nearest neighboring grid points. This is equivalent to the nearest neighbor dynamics as described in the previous chapter. If the selected point is empty, proliferation proceeds. If the selected point is occupied, proliferation does not occur. A proliferating wild-type cell can also incur an additional probability of mutation M, such that the probability of producing an uninfected mutant offspring is PM.

Unlike wild-type proliferation, uninfected mutant cells can only give rise to other uninfected mutants. Data indicates that drug resistance mutations confer a replicative fitness cost in the absence of therapy. Specifically, it has been shown in chronic myeloid leukemia (CML) that drug resistant mutants grow less efficiently than drug sensitive cells [65]. While no other reports exist regarding the relative fitness of drug resistant mutants in cancer, fitness costs of drug resistant mutants have been demonstrated in the past in the context of infectious diseases, particularly in HIV. The fitness cost of drug resistance in HIV tends to be in the range of 1-10 percent, although there are instances of higher fitness costs with some mutations [66]. Here, we assume that the replicative fitness cost for mutant cells here is 10%, such that the probability of proliferation for mutant cells is $0.9P$.

Alternatively, if the chosen grid point is an infected cell, it dies with probability *A.* Again, the cell death will result in an empty grid point into which an uninfected cell can be produced. We assume that infected cells die at a higher rate than uninfected cells (*A>D)* since infected cells can be targeted by the immune system [73]. Infected cells, however, do not reproduce since typical oncolytic viruses lock the cell in S-phase for viral replication, thus preventing any further cellular division [72]. Infected cells transmit the virus with probability *B.* A destination point is chosen randomly from one of the eight nearest neighbors. If the selected grid point contains an uninfected cell, infection proceeds and the target cell becomes infected. Otherwise, infection does not occur. For reference, parameters and their meanings are summarized in Table 4.1.

N	Grid size N x N
P	Probability of uninfected cell proliferation
D	Probability of uninfected cell death
W	Probability of wild-type death following treatment
A	Probability of infected cell death
B	Probability of infecting another cell
M	Probability of mutation

Table 4.1: Parameters for spatial agent based model of oncolytic virus therapy.

4.3 Dynamics of drug resistant versus drug sensitive cancer cells with treatment

We first begin with an initial population of uninfected wild-type cells (5x5 spots), into which we randomly place a small initial population of nine infected wild-type cells.

This takes place in a grid space which overall contains 300 x 300 spots. In the absence of the virus, the population of wild-type cells grows in a quadratic (or “surface” growth) manner, at which point the mutant population arises naturally through mutation. Both cancer cell populations continue to grow, at first quadratically, and then with a slower rate as the number of cells reach higher levels. Once the grid is filled, the two populations of cells approach equilibrium (Fig. 4.1a). In the context of cancer, this means that the cancer has grown to some level at which it can no longer growth without additional mutations. In the presence of the virus, the population of infected wild-type cells grows proportionally as the number of susceptible hosts increases. Since infected cells die at a higher rate than uninfected cells, however, mutant cells may struggle to establish a strong initial population. As the population of infected cells grows, this leads to suppression of the mutant population through apparent competition. Once the population of uninfected mutant cells is driven to extinction by the virus, the population may recover through mutations of the wild-type cell. This leads to a stochastic oscillatory behavior in which the drug resistant mutant is repeatedly driven to extinction before recovering through mutations (Fig. 4.1b). As a result of the virus, the two populations of uninfected cancer cells are maintained at a lower equilibrium than in the absence of the virus. By increasing the probability of infection, and thereby increasing the infection efficiency of the virus, the mutant can be suppressed further, leading to an increase in extinction frequency and a longer duration of extinction (Fig. 4.1c). This is because the overall population of uninfected cancer cells is lower, hence the frequency of generating a resistant mutant is lower. Note, however, that if the probability of infection increases past a certain threshold, the virus alone will eradicate

all populations of cells. Since this is not the focus of this chapter, we do not consider this scenario here.

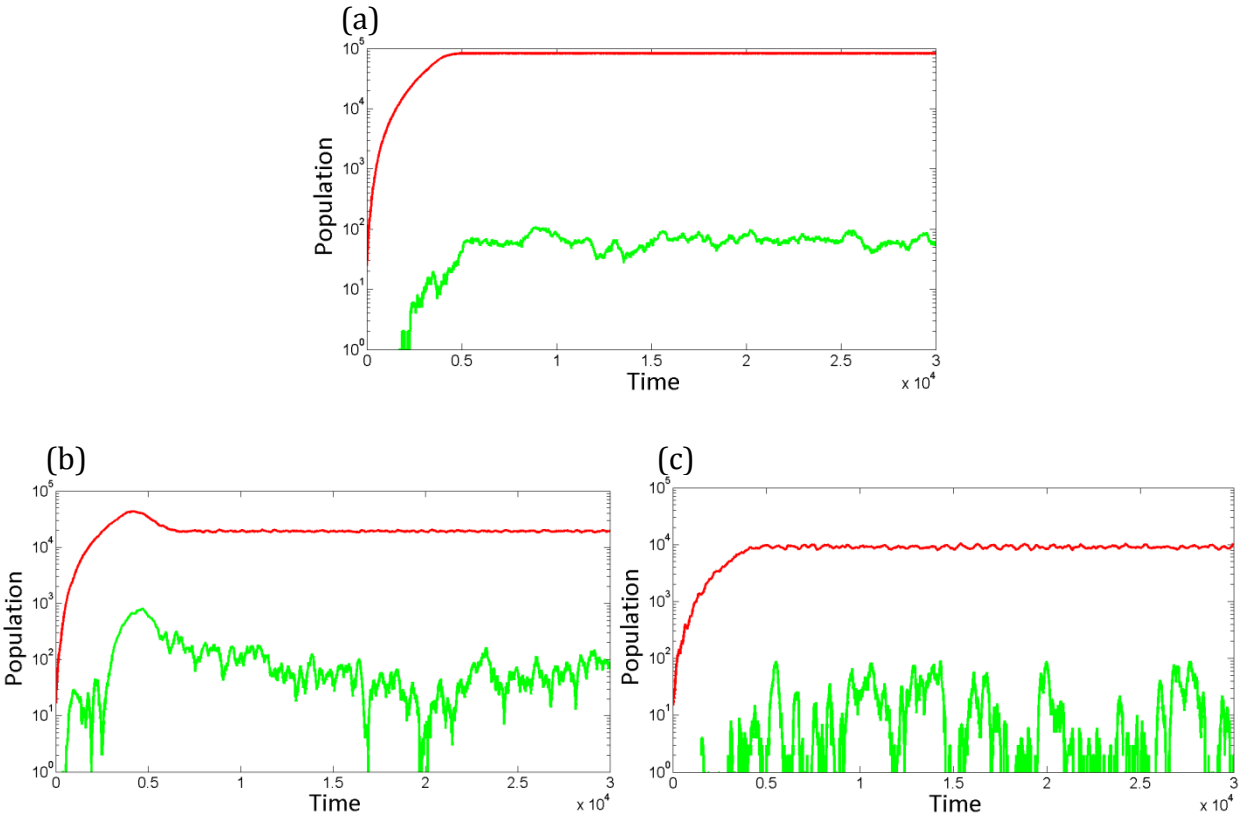

Figure 4.1. The growth of drug sensitive and drug resistant mutants in the (a) absence and (b, c) presence of an oncolytic virus. Red: Drug sensitive wild-type cell. Green: Drug resistant mutant cell. In the absence of the virus (a), the population of drug sensitive wild-type cells grows at first quadratically and then slower as the number of cells approaches equilibrium. Drug resistant mutants arise naturally during the initial quadratic growth phase through mutations. In the presence of the virus (b), the drug sensitive cells grow to a lower equilibrium due to suppression by the virus. The drug resistant mutant, however, is driven to extinction due to apparent competition mediated by the oncolytic virus. The population quickly recovers due to mutations of the drug sensitive cell. The frequency and duration of extinction is amplified when the efficiency of the virus increases (c). The following parameter values were used: N=300, P=0.06, D=0.004, A=0.009, M=10^{-6}, (a) B=0, (b) B=0.06, (c) B=0.12.

The notion that infection efficiency changes the dynamics of apparent competition is especially important in the context of chemotherapy and drug treatment. Here, drug

therapy is modelled by assuming that drug sensitive wild-type cells incur an additional death rate, and are no longer capable of proliferation. Mutant cancer cells are unaffected by drug therapy, and thus do not receive the additional death rate, and are still capable of proliferation. There are two possible outcomes in considering the application of drug therapy once the cancer has grown to equilibrium. If treatment is introduced when the mutant population is at relatively high numbers, the drug sensitive wild-type population declines to extinction, and the drug resistant mutant population grows uncontested (Fig. 4.2a). Drug therapy has failed. However, if treatment is introduced when the drug resistant mutant population is at relatively low numbers or is extinct, the drug sensitive wild-type population declines to extinction and the cancer is eliminated (Fig. 4.2b).

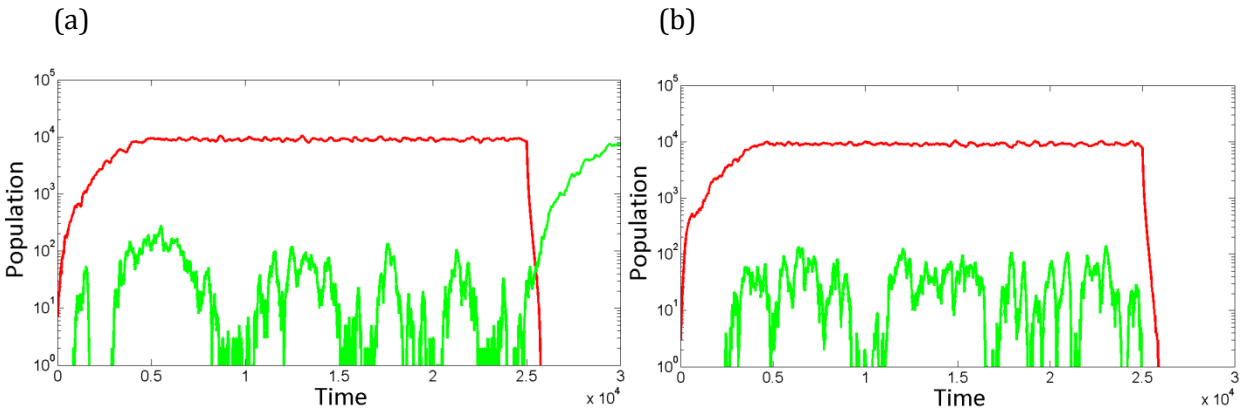

Figure 4.2. Simulation demonstrating the effect of stochasticity on the success of drug therapy. Red: Drug sensitive wild-type cell. Green: Drug resistant mutant cell. It is possible to achieve both drug therapy success and drug therapy failure for the same virus infection rate due to the stochasticity of the system. Here, treatment is applied at twenty-five thousand time steps. If drug therapy is applied while the mutant population is relatively high (a), the drug sensitive population is driven to extinction and the mutant grows uncontested. Here, drug therapy fails. If drug therapy is applied while the mutant population is extinct or too low to recover due to stochasticity (b), drug therapy succeeds and the cancer is eradicated. The following parameter values were used: N=300, P=0.06, D=0.004, A=0.009, M=10^{-6}, B=0.06, W=0.008.

Due to the stochasticity of the system, successes and failures after drug therapy are both observable under identical initial conditions and parameters. The reason for this is as follows. By increasing the efficiency of the virus, apparent competition is increased, leading to more effective suppression of the drug resistant mutant population, and an increase in the duration of time at which the mutant population is extinct (Fig. 4.3a). This is because regrowth of the mutant from low numbers is stochastic, and prone to extinction. If drug therapy is applied while the mutant population is extinct, then extinction of the wild-type population follows and treatment success is observed. If drug therapy is applied while the mutant population greater than zero, the mutant population must recover through its own proliferation since wild-type cells can no longer contribute to the mutant population. Thus, if the mutant population is sufficiently low, high probabilities of infection will prevent the mutant population from recovering, consequently driving it to extinction. As a result, the frequency of success with drug therapy rises with an increase in infection rate (Fig. 4.3b).

This behavior is also observable when we consider only the cases in which the mutant population is non-zero at the start of treatment. In these scenarios, the frequency of success still increases with the probability of infection (Fig. 4.3b). At moderate probabilities of infection, the mutant population displays less stochasticity, maintaining its population at higher levels. This results in an increased likelihood of applying drug therapy when the mutant population is non-zero. As probabilities of infection increase, the likelihood of applying drug therapy when the mutant population is non-zero decreases. However, the frequency of drug therapy success in this scenario continues to increase. This is because an efficient virus is capable of spreading more quickly and bringing the drug resistant mutant population under control.

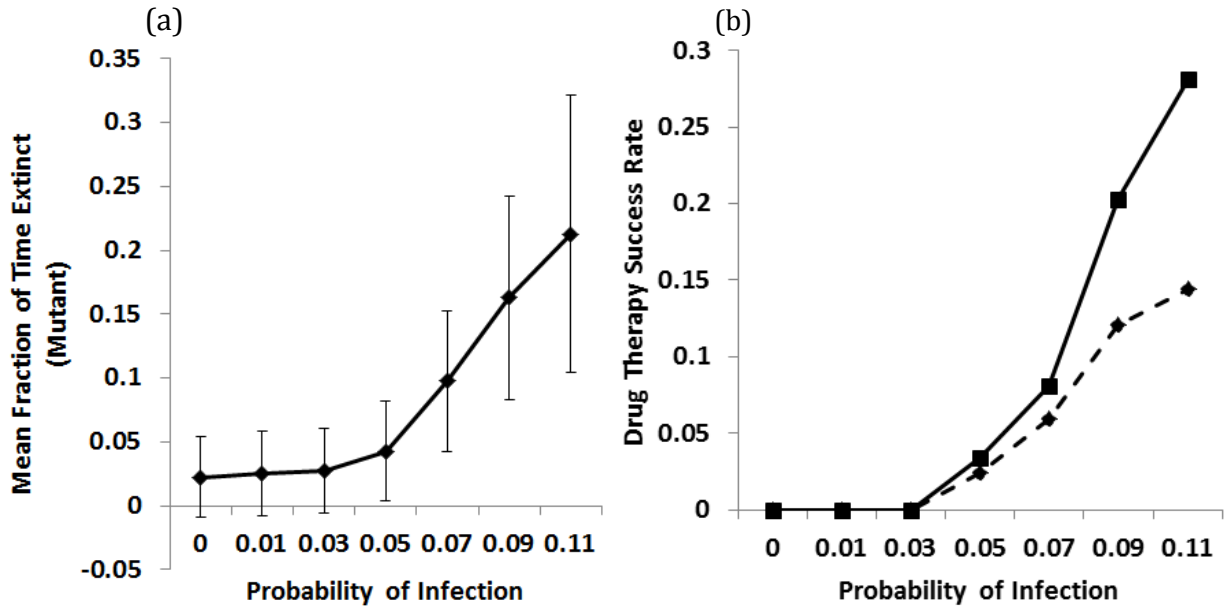

Figure 4.3. The effect of oncolytic virus infection rate on (a) the average fraction of time that the mutant is extinct and (b) the success of drug therapy. (a) The fraction of time the mutant is extinct is calculated by measuring the total duration of extinction from when the mutant first arises until drug therapy is applied. As the probability of infection increases, the less likely it is that the drug resistant mutant will be present in the total cancer population. This is because the size of the cancer is smaller during oncolytic virus therapy, resulting in a decreased probability of generating a mutant. In addition, recovery of the mutant population from low numbers is stochastic, and may be prone to extinction. (b) An increase in the infection rate also results in an increase in the overall frequency of drug therapy success (solid line). This total accounts for treatments applied when the mutant population is temporarily extinct, as well as treatments applied when the mutant population is non-zero. This increase in frequency of success, however, is also observed when only considering treatments applied when the mutant population is non-zero (dashed line). This is because a virus with a higher infection rate is able to spread and control the mutant population for efficiently. The values presented here are based on 1000 simulations for each probability of infection. The following parameter values were used: N=300, P=0.06, D=0.004, A=0.009, M=10^{-6}, W=0.008.

4.4 Combination therapy during early growth phase

The above analysis assumed an initial population containing both uninfected and infected wild-type cells, whereupon drug therapy was applied once the system had reached

a stable equilibrium. However, cancer growth may cause mortality before it reaches a stable population size. We previously observed that the ability of the virus to down-regulate the drug resistant cancer cell population is affected by its infection efficiency. Thus, if the virus spreads too slowly or the cancer grows too quickly, it is possible that the cancer will reach a size which causes mortality before oncolytic viruses or drug therapy can have any effect. However, if oncolytic virus therapy is applied during the growth phase, and the virus limits tumor growth before it reaches a size at which mortality is observed, then oncolytic virus therapy can suppress the drug resistant mutant population, and drug therapy can then be applied.

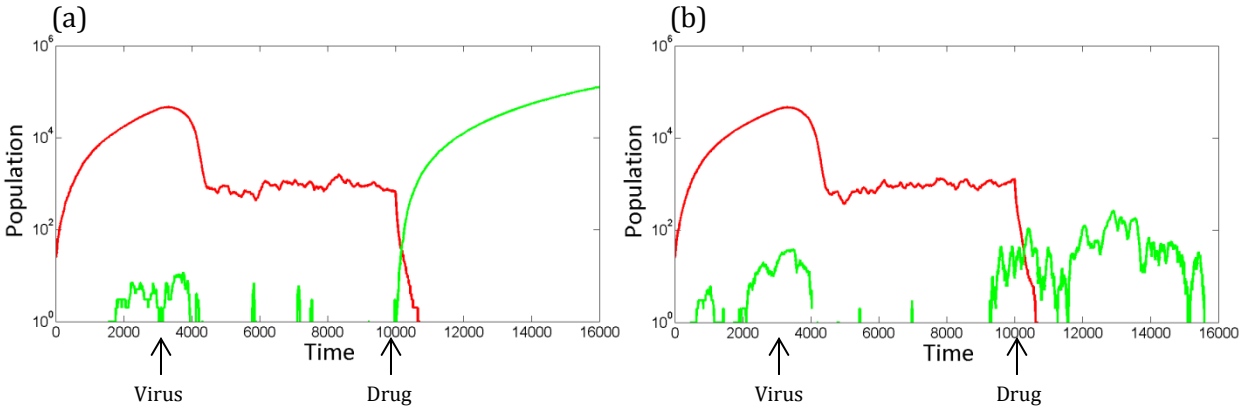

Figure 4.4. Simulation demonstrating the effect of stochasticity on the success of the sequential combination of oncolytic virus therapy and drug treatment during the quadratic growth phase. Red: drug sensitive wild-type cell. Green: drug resistant mutant cell. Here, virus therapy is applied at three thousand time steps, and drug therapy is applied at ten thousand time steps. As before, the drug sensitive wild-type cells initially grow quadratically, with mutants arising naturally through mutation. Once virus therapy is applied, the wild-type cells fall to an equilibrium, while the mutant population is suppressed, recovering from extinction only through mutations of the wild-type. This recovery is prone to extinction due to stochasticity. In addition, the virus population may continue to suppress the mutant population. Thus, both (a) persistence of the mutant population and (b) extinction of the mutant population are possible when drug therapy applied when the mutant population is non-zero. Recovery of the mutants is not possible since there are no wild-type remaining. The following parameter values were used: N=300, P=0.06, D=0.004, A=0.009, M=10^{-6}, B=0.225, W=0.008.

We now consider a grid space containing 1000 x 1000 spots, in which we place an initial population of uninfected wild-type cells (5x5 spots). Here, we use a larger grid space to allow for an increased quadratic growth phase, and a larger equilibrium population size. As before, the population of wild-type cells initially grows in a quadratic manner, at which point the mutant population arises naturally through mutation. If allowed to continue, both cancer cell populations continue to grow, at first quadratically, and then with a slower rate as the number of cells reach higher levels. Once the grid is filled, the two populations of cancer cells approach equilibrium. If oncolytic virus therapy is added during the growth phase, however, the population of infected cells grows, suppressing the population of both drug sensitive wild-type cells and drug resistant mutants to lower levels. Once again, an increase in the population of infected cells leads to an increase in apparent competition. The mutant population must recover through mutations of the wild-type cell once the population of uninfected mutant cells is driven to extinction by the virus.

As before, if drug therapy is applied while the mutant population is extinct, the cancer is eliminated and drug therapy succeeds. Since the oncolytic virus has a suppressive effect on the drug resistant mutant population, applying drug therapy while the infected mutant population is low has several possible outcomes. If drug therapy is applied when the mutant population is relatively high, then the wild-type population is driven to extinction and the drug resistant mutant grows uncontested (Fig. 4.4a). Thus, the sequential combination of oncolytic virus therapy and drug therapy has failed. However, recovery of the mutant population at low numbers is prone to extinction due to stochasticity. This is because the overall population of cancer cells is small with oncolytic virus therapy, leading to a lower probability of generating a drug resistant mutant. In

addition, the oncolytic virus continues to suppress the drug resistant mutant population after drug therapy has driven the drug sensitive wild-type population to extinction (Fig. 4.4b). Since the mutant population can no longer be re-established through mutations of the wild-type cancer cells, any extinction of the mutant caused by the virus is permanent.

Again we note that due to the stochasticity of the system, both drug therapy success and drug therapy failure are possible outcomes for the same initial conditions and parameters. In this section, our analyses of oncolytic virus therapy utilize a parameter regime containing higher probabilities of infection than those of the previous section. This is because oncolytic virus therapy is applied during the quadratic growth phase here, when the population of cells is rapidly increasing. This requires increased virus efficiency in order to suppress the mutant effectively. This increase in probability of infection leads to an increase in the fraction of time in which the mutant is extinct (Fig. 4.5a). As a result, application of drug therapy is more likely to occur when the mutant population is extinct, leading to eradication of the cancer. We also observe that the increase in probability of infection leads to an increase of drug therapy success even when the mutant population is non-zero at the start of treatment. This results in an overall increase in treatment success (Fig. 4.5b).

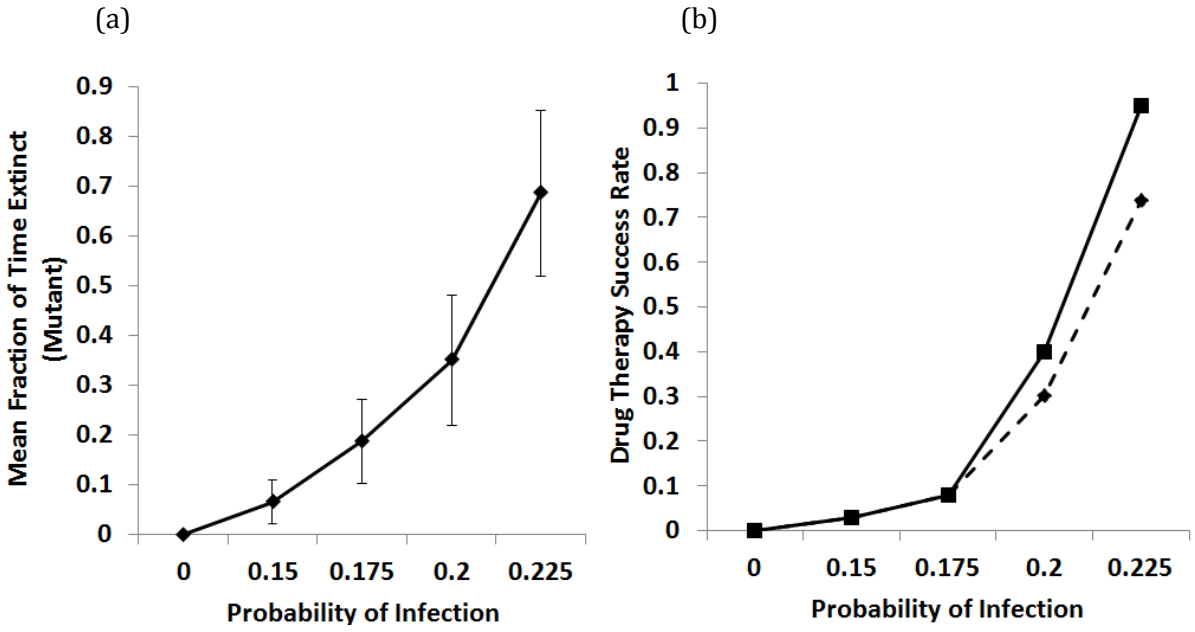

Figure 4.5. The effect of oncolytic virus infection rate on (a) the average fraction of time that the mutant is extinct and (b) the success of drug therapy during the quadratic growth phase. (a) Since virus therapy is applied during the quadratic growth phase, where the population is rapidly increasing, higher probabilities of infection are required to effectively suppress the mutant as compared to the equilibrium simulations previously described. As before, an increase in the probability of infection decreases the likelihood that the drug resistant mutant will be present in the total cancer population. Since higher infection rates are used here, the total cancer population is maintained at a lower equilibrium, leading to a higher fraction of time the mutant remains extinct. (b) An increase in the probability of infection also increases the overall frequency of drug therapy success (solid line). Again, this total accounts for treatments applied when the mutant population is temporarily extinct, as well as treatments applied when the mutant population is non-zero. This increase in frequency of drug therapy success is also observed when considering only treatments applied when the mutant population is non-zero (dashed line). The high fraction of time that the mutant is extinct leads to increased drug therapy success rates compared to the equilibrium simulations described in the previous section. The values presented here are based on 100 simulations for each probability of infection. The following parameter values were used: N=300, P=0.06, D=0.004, A=0.009, M=10^{-6}, W=0.008.

4.5 Discussion and Conclusion

In this chapter we used an agent-based model to investigate a novel way of using oncolytic virus therapy as part of a broader cancer treatment strategy. A particular problem associated with drug therapy is the emergence of drug resistant mutant cells, especially at later stages of cancer. This has led to the exploration of oncolytic viruses as an alternative cancer treatment method. Nonetheless, consistent and sustained eradication of the cancer has not been demonstrated. However, even if the oncolytic virus cannot eradicate the cancer, it may be possible to eradicate the subpopulation of drug resistant mutants, subsequently allowing treatment with drug therapy such as small-molecule inhibitors like Imatinib. An oncolytic virus can be used to 'pretreat' the cancer, suppressing the population of drug resistant cells through a process referred to as 'apparent competition' in the ecological literature [64]. This is made possible because drug resistance mutations incur a replicative fitness cost compared to drug sensitive cells. Such fitness costs in the context of cancer have been observed in CML [65]. Drug resistance mutations have also been demonstrated convincingly in the context of HIV, where the fitness cost of drug resistance often manifests itself in a 1-10 percent replicative fitness cost [66]. While the association of fitness costs and drug resistance mutations is likely to be a general phenomenon, more experimental research needs to be done in the context of cancer.

Our method of using an agent-based model expanded on previous models by allowing for stochastic and spatial interactions, elements found in nature but typically lacking in systems based on ordinary differential equations. We found that the presence of the oncolytic virus suppresses the population of drug resistant mutant cells through

apparent competition. Once cells become infected, they die at a higher rate than uninfected cells. Consequently, the drug resistant mutant population can be driven to extinction. Nevertheless, the mutant population may recover through mutations of the wild-type cells. This has important implications for drug therapy. If drug therapy is applied when the mutant population is recovered and established, the drug-sensitive population is driven to extinction and the drug resistant mutant grows uncontested. In this case drug therapy has failed. If drug therapy is applied when the mutant population is extinct or too low to recover, the cancer is eradicated and treatment has succeeded. One possible reason is that the size of the cancer is smaller with oncolytic virus therapy, hence the probability generating a drug resistant mutant is lower [74]. In addition, the recovery of the mutant population from low numbers is stochastic, and prone to extinction. As a result, the frequency of treatment success depends heavily on the infection efficiency of the virus. An increase in the efficiency of the virus leads to a decrease in the overall cancer population, more effective suppression of the drug resistant mutant, and subsequently a higher frequency of treatment success.

Note that this treatment strategy differs from the simultaneous combination of oncolytic virus therapy and drug therapy [75-78]. These types of strategies aim to reduce the replicative ability of the cancer, allowing for more effective virus mediated-eradication. In the context of drug resistant mutants, however, this could be dangerous. This is because drug resistant mutants have a replicative advantage in the presence of drug therapy. As a result, apparent competition through the oncolytic virus would lead to suppression of the drug sensitive population instead. This would ultimately allow the drug resistant mutants to grow to high levels uncontested. Rather, our approach utilizes the sequential

combination of oncolytic virus therapy and drug therapy. Here, we capitalize on the replicative advantage that drug sensitive cells have in the absence of drug therapy to suppress the drug resistant mutants through apparent competition. This is followed by drug therapy with the aim of eradicating the cancer.

In addition, there are arguments and assumptions presented in this chapter that do not take into account other complicating factors that may affect successful oncolytic virus therapy and drug treatment. For example, since chemotherapeutic drugs targets cells that are highly proliferative, quiescent cancer cells may not be affected by the drug [79]. Even in the absence of drug resistant mutants, this can pose a significant obstacle. Furthermore, quiescent cells are unlikely to produce much virus if infected since the oncolytic virus replicates through utilizing the host cells active machinery. Another important assumption of our model is that all uninfected cancer cells are susceptible to virus infection. However, it is possible that some cancer cells have reduced levels of surface receptors necessary for viral entry, effectively rendering them resistant to the virus [80]. In addition, cells may become temporarily resistant to virus-induced effects depending on the stage of the cell cycle [81]. Here, apparent competition would be incapable of driving the drug resistant mutant population extinct. Such details could be incorporated into future models once we have developed a better understanding of the concepts presented here in the context of specific cancers and oncolytic viruses and their specific properties. Finally, while our model incorporates spatial characteristics not capture by ordinary differential equations, the spatial complexity of tumor growth and virus infection dynamics is enormous and not well understood. For example, our model assumes a virus infection range that consists of the eight nearest neighboring target cells, although this does not have to be true.

In summary, we utilized an agent-based model to investigate a cancer treatment strategy in which oncolytic viruses might be used to drive drug resistant cancer cells extinct, allowing for subsequent eradication of the remaining drug sensitive cancer population through drug therapy. Many biological details must be incorporated into the model for a more detailed analysis, several of which have been discussed. We also have limited knowledge of drug resistance mutations and feasible oncolytic viruses. However, our model is based on the principles of population dynamics and biologically reasonable assumptions, and could be investigated experimentally. For instance, both a drug-sensitive cancer population and drug resistant cancer population could be allowed to grow together in a simple *in vivo* system. This could be followed by the introduction of oncolytic viruses and subsequent drug therapy. The populations of drug resistant and drug sensitive cancer cells should be monitored over time. The experimental results that follow can be compared with model behavior, and can help guide future model revisions and experimental design.

Chapter 5

Summary and Conclusions

In this dissertation we explore the mathematical and computational modeling of virus infection dynamics in two different contexts: the multiple infection of cells by virus, and the use of oncolytic viruses for the eradication of drug resistant cancer cells. In order to achieve this, we utilize systems of ordinary differential equations as well as stochastic agent-based models.

In chapter two, we investigate the difficulties and pitfalls associated with the modeling of multiple infection of cells by viruses using models based on systems of ordinary differential equations. Such models subdivide the total population of infected cells into subpopulations of cells infected by i viruses. In principal, each subpopulation can be further infected to contain $i+1$ viruses. This is referred to as the "multiple infection cascade." In order to study these systems numerically, however, the infection cascade of these models must be artificially truncated, and this can have an effect on the simulation results. If the replication rate of the virus is sufficiently fast, then most infected cells accumulate in the last member of the infection cascade. As a result, the subpopulation

infected cells at the end of the infection cascade becomes over-represented along the distribution of infected cell subpopulations, leading to incorrect numerical results.

In chapter three, we extend this model to account for two different virus types/strains, and investigate how the length of the infection cascade can affect simulation results in the context of virus competition dynamics. We observe that the length of the infection cascade can influence the equilibrium populations in numerical simulations. More specifically, competitive exclusion can be observed for shorter infection cascades, while coexistence can be observed for longer infection cascades. We then examine the model in a parameter regime in which the cascade length does not affect simulation results. Here, we investigate the effect of multiple infections on the outcome of competition. In this context, we observe that multiple infection can promote the coexistence of two competing virus strains if there is an appropriate degree of intracellular niche separation. Finally, we utilize a spatial model to demonstrate that multiple infection has a reduced ability to allow coexistence if virus infection dynamics are spatially restricted compared to perfect mixing mass action scenarios.

In chapter four, we utilize an agent-based model to investigate the use of oncolytic viruses for the eradication of drug resistant cancer cells in the context of space and stochasticity. While clinical trials have not demonstrated a clear success in the eradication of cancer using oncolytic viruses, we observe that it may be possible to eradicate the subpopulation of drug resistant cells, leaving only the subpopulation of drug sensitive cells to be treated using drug therapy. Since populations of drug resistant mutants cells can be regenerated by mutations of drug sensitive cells, the infection efficiency of the virus has an

effect on the success rate of the subsequent drug therapy. More specifically, as the infection efficiency of the oncolytic virus increases, the success rate of drug therapy increases as well due to effective suppression of the mutant population by the virus.

Thus, this dissertation and its analyses are important because they address some of the limitations associated with many of the mathematical and computational models of host-pathogen interactions, while providing additional insights. The insights derived here can provide the framework for more detailed explorations, theoretically and experimentally, of other complexities that are relevant for disease dynamics and host-pathogen dynamics *in vivo*.

References

[1] M.A. Nowak, and R.M. May, Virus dynamics. Mathematical principles of immunology and virology., Oxford University Press, 2000.

[2] A.S. Perelson, Modelling viral and immune system dynamics. Nature Rev Immunol **2** (2002) 28-36.

[3] A.S. Perelson, and R.M. Ribeiro, Modeling the within-host dynamics of HIV infection. BMC Biol **11** (2013) 96.

[4] A. Hofacre, D. Wodarz, N.L. Komarova, and H. Fan, Early infection and spread of a conditionally replicating adenovirus under conditions of plaque formation. Virology **423** (2012) 89-96.

[5] J. Chen, Q. Dang, D. Unutmaz, V.K. Pathak, F. Maldarelli, D. Powell, and W.S. Hu, Mechanisms of nonrandom human immunodeficiency virus type 1 infection and double infection: preference in virus entry is important but is not the sole factor. J Virol **79** (2005) 4140-9.

[6] Q. Dang, J. Chen, D. Unutmaz, J.M. Coffin, V.K. Pathak, D. Powell, V.N. KewalRamani, F. Maldarelli, and W.S. Hu, Nonrandom HIV-1 infection and double infection via direct and cell-mediated pathways. Proc Natl Acad Sci U S A **101** (2004) 632-7.

[7] D.N. Levy, G.M. Aldrovandi, O. Kutsch, and G.M. Shaw, Dynamics of HIV-1 recombination in its natural target cells. Proc Natl Acad Sci U S A **101** (2004) 4204-9.

[8] W. Hubner, G.P. McNerney, P. Chen, B.M. Dale, R.E. Gordon, F.Y. Chuang, X.D. Li, D.M. Asmuth, T. Huser, and B.K. Chen, Quantitative 3D video microscopy of HIV transfer across T cell virological synapses. Science **323** (2009) 1743-7.

[9] A. Jung, R. Maier, J.P. Vartanian, G. Bocharov, V. Jung, U. Fischer, E. Meese, S. Wain-Hobson, and A. Meyerhans, Multiply infected spleen cells in HIV patients. Nature **418** (2002) 144.

[10] L. Josefsson, M.S. King, B. Makitalo, J. Brannstrom, W. Shao, F. Maldarelli, M.F. Kearney, W.S. Hu, J. Chen, H. Gaines, J.W. Mellors, J. Albert, J.M. Coffin, and S.E. Palmer, Majority of CD4+ T cells from peripheral blood of HIV-1-infected individuals contain only one HIV DNA molecule. Proc Natl Acad Sci U S A **108** (2011) 11199-204.

[11] L. Josefsson, S. Palmer, N.R. Faria, P. Lemey, J. Casazza, D. Ambrozak, M. Kearney, W. Shao, S. Kottilil, M. Sneller, J. Mellors, J.M. Coffin, and F. Maldarelli, Single cell

analysis of lymph node tissue from HIV-1 infected patients reveals that the majority of CD4+ T-cells contain one HIV-1 DNA molecule. PLoS Pathog **9** (2013) e1003432.

[12] R.A. Neher, and T. Leitner, Recombination rate and selection strength in HIV intra-patient evolution. PLoS Comput Biol **6** (2010) e1000660.

[13] N.M. Dixit, and A.S. Perelson, HIV dynamics with multiple infections of target cells. Proc Natl Acad Sci U S A **102** (2005) 8198-203.

[14] N.M. Dixit, and A.S. Perelson, Multiplicity of human immunodeficiency virus infections in lymphoid tissue. J Virol **78** (2004) 8942-5.

[15] D. Wodarz, and D.N. Levy, Effect of different modes of viral spread on the dynamics of multiply infected cells in human immunodeficiency virus infection. J R Soc Interface **8** (2011) 289-300.

[16] K.W. Cummings, D.N. Levy, and D. Wodarz, Increased burst size in multiply infected cells can alter basic virus dynamics. Biol Direct **7** (2012) 16.

[17] M.T. Bretscher, C.L. Althaus, V. Muller, and S. Bonhoeffer, Recombination in HIV and the evolution of drug resistance: for better or for worse? Bioessays **26** (2004) 180-8.

[18] C. Fraser, HIV recombination: what is the impact on antiretroviral therapy? J R Soc Interface **2** (2005) 489-503.

[19] R.D. Kouyos, S.P. Otto, and S. Bonhoeffer, Effect of varying epistasis on the evolution of recombination. Genetics **173** (2006) 589-97.

[20] D. Wodarz, and D.N. Levy, Human immunodeficiency virus evolution towards reduced replicative fitness in vivo and the development of AIDS. Proc Biol Sci **274** (2007) 2481-90.

[21] D. Wodarz, and D.N. Levy, Multiple HIV-1 infection of cells and the evolutionary dynamics of cytotoxic T lymphocyte escape mutants. Evolution **63** (2009) 2326-39.

[22] K. Dietz, Epidemiologic Interference of Virus Populations. Journal of Mathematical Biology **8** (1979) 291-300.

[23] S. Gupta, J. Swinton, and R.M. Anderson, Theoretical-Studies of the Effects of Heterogeneity in the Parasite Population on the Transmission Dynamics of Malaria. Proceedings of the Royal Society of London Series B-Biological Sciences **256** (1994) 231-238.

[24] M. Lipsitch, Vaccination against colonizing bacteria with multiple serotypes. Proceedings of the National Academy of Sciences of the United States of America **94** (1997) 6571-6576.

[25] J. Mosquera, and F.R. Adler, Evolution of virulence: a unified framework for coinfection and superinfection. Journal of Theoretical Biology **195** (1998) 293-313.

[26] M.A. Nowak, and R.M. May, Superinfection and the evolution of parasite virulence. Proc R Soc Lond B Biol Sci **255** (1994) 81-9.

[27] M. Lipsitch, C. Colijn, T. Cohen, W.P. Hanage, and C. Fraser, No coexistence for free: neutral null models for multistrain pathogens. Epidemics **1** (2009) 2-13.

[28] M. vanBaalen, and M.W. Sabelis, The dynamics of multiple infection and the evolution of virulence. American Naturalist **146** (1995) 881-910.

[29] D. Wodarz, Ecological and evolutionary principles in immunology. Ecol Lett **9** (2006) 694-705.

[30] C.L. Ball, M.A. Gilchrist, and D. Coombs, Modeling within-host evolution of HIV: mutation, competition and strain replacement. Bull Math Biol **69** (2007) 2361-85.

[31] D. Coombs, M.A. Gilchrist, and C.L. Ball, Evaluating the importance of within- and between-host selection pressures on the evolution of chronic pathogens. Theor Popul Biol **72** (2007) 576-91.

[32] M. Begon, C.R. Townsend, and J.L. Harper, Ecology: from individuals to ecosystems. (2006).

[33] N.L. Komarova, D.N. Levy, and D. Wodarz, Effect of synaptic transmission on viral fitness in HIV infection. PLoS One **7** (2012) e48361.

[34] V. Malhotra and M.C. Perry, Classical chemotherapy: mechanisms, toxcities, and the therapeutic window. Cancer Biol Ther **2** (2003) S2-4.

[35] P.G. Corrie and G. Pippa, Cytotoxic chemotherapy: clinical aspects. Medicine **36** (2008) 24-28.

[36] K.W. Yee and A. Keating, Advances in targeted therapy for chronic myeloid leukemia. Exepert Rev Anticancer Ther **3** (2003) 295-310.

[37] V. Guillemard and H.U. Saragovi, Novel approaches for targeted cancer therapy. Curr CancerDrug Targets **4** (2004) 313-326.

[38] E.A. Harrington, D. Bebbington, J. Moore, R.K. Rasmussen, A.O. Ajose-Adeogun, et al. VX-680, a potent and selective small-molecule inhibitor of the Aurora kinases, supresses tumor growth in vivo. Nature Medicine **10** (2004) 262-267.

[39] J. Zhang, P.L. Yang, and N.S. Gray, Targeting cancer with small molecule kinase inhibitors. Nature Reviews Cancer **9** (2009) 28-39.

[40] C.L. Sawyers, Chronic myeloid leukemia. N Engl J Med **340** (1999) 1330-1340.

[41] M.W. Deininger, J.M. Goldman, and J.V. Melo, The molecular biology of chronic myeloid leukemia. Blood **96** (2000) 3343-3356.

[42] M.D. Moen, K. McKeage, G.L. Plosker, and M.A. Siddiqui, Imatinib: a review of its use in chronic myeloid leakaemia. Drugs **2** (2007) 299-320.

[43] M. Henkes, H. van der Kuip, W.E. Aulitzky, Therapeutic options for chronic myeloid leukemia: focus on imatinib. Ther Clin Risk Manag **4** (2008) 163-187.

[44] B.D. Smith, Imatinib for chronic myeloid leukemia: the impact of its effectiveness and long term side effects. J Natl Cancer Inst (2011).

[45] M.E. Gorre, M. Mohammed, K. Ellwood, N. Hsu, R. Paquette, P.N. Rao, and C.L. Sawyers, Clinical resistant to STI-571 cancer therapy caused by BCR-ABL gene mutation or amplification. Science **293** (2001) 876-880.

[46] K.M. Shannon, Resistance in the land of molecular cancer therapeutics. Cancer Cell **2** (2002)99-102.

[47] J.M. Goldman and J.V. Melo, Chronic myeloid leukemia – advances in biology and new approaches to treatment. N Engl J Med **349** (2003) 1451-1464.

[48] J.V. Melo and D.J. Barnes, Chronic myeloid leukaemia as a model of disease evolution in human cancer. Nat Rev Cancer **7** (2007) 441-453.

[49] D.S. Tan, M. Gerlinger, B.T. Teh, and C. Swanton, Anti-cancer drug resistance: understanding the mechanisms through the use of integrative genomics and functional RNA interference. European Journal of Cancer **46** (2010) 2166-2177.

[50] M. Shanker, D. Wullcutts, J.A. Roth, and R. Ramesh, Drug resistant in lung cancer. Lung Cancer: Targets and Therapy **1** (2010) 23-26.

[51] N.A. Saunders, F. Simpson, E.W. Thompson, M.M. Hill, L. Endo-Munoz, G. Leggatt, R.F. Minchin, and A. Guminski, Role of intratumoural heterogeneity in cancer drug resistant: molecular and clinical perspectives. EMBO Mol Med **4** (2012) 674-684.

[52] M. Aghi and R.L. Martuza, Oncolytic viral therapies – the clinical experience. Oncogene 24 (2005) 7802-7816.

[53] V. Beljanski and J. Hiscott, The use of oncolytic viruses to overcome lung cancer drug resistance. Current Opinion in Virology **2** (2012) 629-635.

[54] J.J. Davis and B. Fang, Oncolytic virotherapy for cancer treatment: challenges and solutions. J Gene Med **7** (2005) 1380-1389.

[55] J.C. Bell, Oncoloytic viruses: what's next? Curr. Cancer Drug Targets **7** (2007) 127-131.

[56] A.M. Crompton and D.H. Kirn, From ONYX-015 to armed vaccinia viruses: the education and evolution of oncolytic virus development. Curr Cancer Drug Targets **7** (2007) 133-139.

[57] N.G. Chen, A. A. Szalay, R.M. Buller, and U.M. Lauer, Oncolytic viruses. Advances in Virology. 320206.

[58] M. Bauzon and T.W. Hermiston, Oncolytic viruses: the power of directed evolution. Advances in Virology (2012) 586389.

[59] R. Auer and J.C. Bell, Oncolytic viruses: smart therpeutics for smart cancers. Future Oncology **8** (2012) 1-4

[60] K. Garber, China approves world's first oncolytic virus therapy for cancer treatment. J Natl Cancer Inst **98** (2006) 298-300.

[61] C. Croce, Oncogenes and cancer, N Engl J Med **358** (2008) 502-511.

[62] H.H. Wong, N.R. Lemoine, and Y. Wang, Oncolytic viruses for cancer therapy: overcoming the obstacles. Viruses **2** (2010) 78-106.

[63] D. Wodarz, Use of oncolytic viruses for the eradication of drug-resistant cancer cells. J R Soc Interface **6** (2009) 179-186.

[64] R.D. Holt, Predation, apparent competition and the structure of prey communitites. Theor Popul Biol **12** (1977) 197-229.

[65] A.J. Tipping, F.X. Mahon, V. Lagarde, J.M. Goldman, and J.V. Melo. Restoration of sensitivity to STI571 in STI571-resistant chronic myeloid leukemia cells. Blood **98** (2001) 3864-3867.

[66] N.K. Back, M. Nijhuis, W. Keulen, C.A. Boucher, B.O. Oude Essink, A.B. van Kuilenburg, A.H. van Gennip, and B. Berkhout, Reduced replication of 3TC-resistant HIV-1 variants in primary cells due to a processivity defect of the reverse transcriptase enzyme. Embo J **15** (1996) 4040-4049.

[67] D. Wodarz, Viruses as antitumor weapons: defining conditions for tumor remission. Cancer Res **61** (2001) 3501-3507.

[68] D. Wodarz, Gene therapy for killing p-53-negative cancer cells: use of replicating versus nonreplicating agents. Hum Gene Ther **14** (2003) 153-159.

[69] D. Dingli, M.D. Cascino, K. Josic, S.J. Russell, and Z. Bajzer, Mathematical modeling of cancer radiovirotherapy. Math Biosci **199** (2006) 55-78.

[70] Z. Bajzer, T. Carr, K. Josic, S.J. Russell, and D. Dingli, Modeling of cancer virotherapy with recombinant measles viruses. J Theor Biol **252** (2008) 109-122.

[71] N.L. Komarova and D. Wodarz, ODE models for oncolytic virus dynamics. J Theor Biol **263** (2010) 530-543.

[72] N. Bagheri, M. Shiina, D.A. Lauffenburger, and W. Michael Korn, A dynamical systems model for combinatorial cancer therapy enhances oncolytic adenovirus efficacy by MEK inhibition. PLoS Comput Biol **7** (2011) e1001085.

[73] D. Wodarz, Killer cell dynamics. Springer Science (2007).

[74] D. Wodarz and N.L. Komarova, Emergence and prevention of resistance against small molecule inhibitors. Semin Cancer Biol **15** (2005) 506-514.

[75] L. You, C.T. Yang, D.M Jablons, ONYX-015 works synergistically with chemotherapy in lung cancer lines and primary cultures freshly made from lung cancer patients. Cancer Research **60** (2000) 1009-1013.

[76] H.S. Pandha, L. Heinemann, G.R. Simpson, A. Melcher, R. Prestwich, F. Errington, M. Coffey, K.J. Harrington, and R. Morgan, Synergistic effects of oncolytic reovirus and cisplatin chemotherapy in murine malignant melanoma. Clin Cancer Res **19** (2009) 6158-6166.

[77] S. Zhong, D. Yu, Y. Wang, S. Qiu, S. Wu, and X.Y. Liu, Synergistic antitumor effect of TRAIL and IL-24 with complete eradication of hepatoma in the CTGVT-DG strategy. Acta Biochimica et Biophysica Snicia (Shanghai) **44** (2012) 535-543.

[78] E. Hofmann, W. Weibel, and A.A. Szalay, Combination treatment with oncolytic vaccinia virus and cyclophosphamide results in synergistic antitumor effects in human lung adenocarcinoma. Journal of Translational Medicine **12** (2014) 197.

[79] T. Holyoake, X. Jiang, C. Eaves, and A. Eaves, Isolation of a highly quiescent subpopulation of primitive leukemic cells in chronic myeloid leukemia. Blood **94** (1999)2056-2064.

[80] W.M. Korn, M. Macal, C. Christian, M.D. Lacher, A. McMillan, et al. Expression of the coxsackievirus and adenovirus receptor in gastrointestinal cancer correlates with tumor differentiation. Cancer Gene Ther **13** (2006) 792-797.

[81] F.D. Goodrum and D.A. Ornelles, The early region 1B 55-kilodalton oncoprotein of adenovirus relieves growth restrictions imposed on viral replication by the cell cycle. J Virol **71** (1997) 548-561.